1 **Biogenic volatile organic compound ambient mixing ratios and emission rates**

2 **in the Alaskan Arctic tundra**

3 **Hélène Angot[1], Katelyn McErlean[1], Lu Hu[2], Dylan B. Millet[3], Jacques Hueber[1], Kaixin Cui[1], Jacob Moss[1],**

4 **Catherine Wielgasz[2], Tyler Milligan[1], Damien Ketcherside[2], Marion Syndonia Bret-Harte[4], Detlev Helmig[1]**

5 [1]Institute of Arctic and Alpine Research, University of Colorado Boulder, Boulder, CO, USA.

6 [2]Department of Chemistry and Biochemistry, University of Montana, Missoula, MT, USA.

7 [3]Department of Soil, Water, and Climate, University of Minnesota, Minneapolis-Saint Paul, MN, USA.

8 [4]Institute of Arctic Biology, University of Alaska-Fairbanks, Fairbanks, Alaska, USA.

9

10 **Abstract**

11 Rapid Arctic warming, a lengthening growing season, and increasing abundance of biogenic volatile

12 organic compounds (BVOC)-emitting shrubs are all anticipated to increase atmospheric BVOCs in the

13 Arctic atmosphere, with implications for atmospheric oxidation processes and climate feedbacks.

14 Quantifying these changes requires an accurate understanding of the underlying processes driving BVOC

15 emissions in the Arctic. While boreal ecosystems have been widely studied, little attention has been paid to

16 Arctic tundra environments. Here, we report terpenoid (isoprene, monoterpenes, and sesquiterpenes)

17 ambient mixing ratios and emission rates from key dominant vegetation species at Toolik Field Station

18 (TFS; 68°38'N, 149°36'W) in northern Alaska during two back-to-back field campaigns (summers 2018

19 and 2019) covering the entire growing season. Isoprene ambient mixing ratios observed at TFS fell within

20 the range of values reported in the Eurasian taiga (0-500 pptv), while monoterpene and sesquiterpene

21 ambient mixing ratios were respectively close to and below the instrumental quantification limit (~2 pptv).

22 Isoprene surface emission rates ranged from 0.2 to 2250 $\mu gC/m^2/h$ (mean of 85 $\mu gC/m^2/h$) and monoterpene

23 emission rates remained on average below 1 $\mu gC/m^2/h$ over the course of the study. We further quantified

24 the temperature dependence of isoprene emissions from local vegetation including *Salix* spp. (a known

25 isoprene emitter), and compared the results to predictions from the Model of Emissions of Gases and

26 Aerosols from Nature version 2.1 (MEGAN2.1). Our observations suggest a 180-215% emission increase

27 in response to a 3-4°C warming and the MEGAN2.1 temperature algorithm exhibits a close fit with

28 observations for enclosure temperatures in the 0-30°C range. The data presented here provide a baseline to

29 investigate future changes in the BVOC emission potential of the under-studied Arctic tundra environment.

1. Introduction

As a major source of reactive carbon to the atmosphere, biogenic volatile organic compounds (BVOCs) emitted from vegetation play a significant role in global carbon and oxidation cycles (Fehsenfeld et al., 1992). Global emission estimates of BVOCs are in the range of 700-1100 TgC per year, ~70-80% of which corresponds to terpenoid species: isoprene, monoterpenes (MT), and sesquiterpenes (SQT) (Guenther et al., 1995, 2006; Sindelarova et al., 2014). Despite their relatively short atmospheric lifetimes (1 hour to 1 day for terpenoids), BVOCs affect climate through their effects on the hydroxyl radical (OH, which dictates the lifetime of atmospheric methane), tropospheric ozone (O_3, a key greenhouse gas), and aerosols (which influence radiative scattering) (Arneth et al., 2010; Fuentes et al., 2000; Peñuelas and Staudt, 2010). The oxidation of those BVOCs also drives the formation of secondary organic aerosols (SOA) through both gas- and aqueous-phase mechanisms (Carlton et al., 2009; Lim et al., 2005). The potential for increased SOA formation, expected to result in climate cooling (Kulmala et al., 2004), complicates the climate feedbacks of BVOC emissions (Tsigaridis and Kanakidou, 2007; Unger, 2014).

Global models of BVOC emissions assume minimal emissions from the Arctic due to low leaf area index and relatively cold temperatures (Guenther et al., 2006; Sindelarova et al., 2014). However, this assumption relies on few observations and has been increasingly challenged by field data (Tang et al., 2016). Recent measurements have revealed significant BVOC emissions from Arctic tundra and vegetation, including *Sphagnum* mosses, wetland sedges, and dwarf shrubs (Ekberg et al., 2009, 2011; Faubert et al., 2010; Holst et al., 2010; Lindfors et al., 2000; Potosnak et al., 2013; Rinnan et al., 2011; Schollert et al., 2014; Tiiva et al., 2008). These results are of importance because BVOC emissions are expected to increase in the Arctic due to climate warming and associated vegetation and land cover change (Faubert et al., 2010; Potosnak et al., 2013; Rinnan et al., 2011; Tiiva et al., 2008). Field warming studies have shown strong increases in BVOC emissions from shrub heath (Michelsen et al., 2012; Tiiva et al., 2008). Furthermore, the temperature dependence of Arctic BVOC fluxes appears to be significantly greater than for tropical and subtropical ecosystems (Holst et al., 2010; Rinnan et al., 2014), with up to 2-fold increases in MT emissions and 5-fold increases in SQT emissions by subarctic heath for a 2°C warming (Valolahti et al., 2015). Similarly, Kramshøj et al. (2016) and Lindwall et al. (2016) examined the response of BVOC emissions to an experimental 3-4°C warming and reported a 260-280%

60   increase in total emissions. Together, the above results emphasize the strong temperature
61   sensitivity of BVOC emissions from Arctic ecosystems.

62   Changing BVOC emissions in the Arctic due to climate and land cover shifts can thus be expected
63   to perturb the overall oxidative chemistry of the region. Previous studies have hypothesized that
64   BVOCs might already impact the diurnal cycle of ozone in the Arctic boundary layer (Van Dam
65   et al., 2016). Changing BVOC emissions can also further affect climate through various feedback
66   mechanisms; Quantifying these changes requires an accurate understanding of the underlying
67   processes driving BVOC emissions in the Arctic. While BVOC ambient mixing ratios and
68   emission rates have been studied in boreal ecosystems, less attention has been paid to Arctic tundra
69   environments (Lindwall et al., 2015). Here, we report BVOC ambient mixing ratios and emission
70   rates at Toolik Field Station (TFS) in the Alaskan Arctic. This study builds on the previous
71   isoprene study at TFS by Potosnak et al. (2013), while also providing a major step forward from
72   that work. In particular, we present the first continuous summertime record of ambient BVOCs
73   (including isoprene and MT) and their first-generation oxidation products in the Arctic tundra
74   environment. The data presented here provide a baseline to investigate future changes in the BVOC
75   emission potential of the under-studied Arctic tundra environment. Due to increasing shrub
76   prevalence across northern Alaska (Berner et al., 2018; Tape et al., 2006), as well as the Eurasian
77   (Macias-Fauria et al., 2012) and Russian Arctic (Forbes et al., 2010), the results of this study have
78   significance to tundra ecosystems across a vast region of the Arctic. We further compare the
79   observed temperature dependence of isoprene emissions with predictions from the Model of
80   Emissions of Gases and Aerosols from Nature version 2.1 (MEGAN2.1), a widely used modeling
81   framework for estimating ecosystem-atmosphere BVOC fluxes (Guenther et al., 2012).

82   **2. Material and Methods**
83   **2.1 Study site**

84   This study was carried out at TFS, a Long-Term Ecological Research (LTER) site located in the
85   tundra on the north flank of the Brooks Range in northern Alaska (68°38'N, 149°36'W; see Fig.1).
86   Vegetation speciation and dynamics, and their changes over time, have been well documented at
87   the site. *Betula* (birch) and *Salix* (willow) are the most common deciduous shrubs (Kade et al.,
88   2012). Common plant species include *Betula nana* (dwarf birch), a major player in ongoing Arctic
89   greening (Hollesen et al., 2015; Sistla et al., 2013), *Rhododendron tomentosum* (formerly *Ledum*

90   *palustre*; Labrador tea); *Vaccinium vitis-idaea* (lowbush cranberry), *Eriophorum vaginatum*

91   (cotton grass), *Sphagnum angustifolium* (peat moss), *Alectoria ochroleuca* (witches hair lichen),

92   and many other perennial species of Carex, mosses, and lichens. Vegetation cover at this site is

93   classified as tussock tundra (see Fig.1), which is the most common vegetation type in the northern

94   foothills of the Brooks Range (Elmendorf et al., 2012; Kade et al., 2012; Shaver and Chapin, 1991;

95   Survey, 2012; Walker et al., 1994).

96   Emission measurements and atmospheric sampling were conducted from a weatherproof

97   instrument shelter located ~350 m to the west of TFS (see Fig.S.I.1). Winds at TFS are

98   predominantly from the southerly and northerly sectors (Toolik Field Station Environmental Data

99   Center, 2019), minimizing any influence from camp emissions at the site. Two field campaigns

100   were carried out: the first from mid-July to mid-August 2018, and the second from mid-May to

101   the end of June 2019. These two back-to-back campaigns cover the entire growing season (Sullivan

102   et al., 2007), from the onset of snow melt mid-May to the first snow fall mid-August.

103   **2.2 Ambient online measurements of BVOCs and their oxidation products**

104   2.2.1   Gas chromatography and mass spectrometry with flame ionization detector

105   (GC-MS/FID)

106   An automated GC-MS/FID system was deployed for continuous measurements of atmospheric

107   BVOCs at ~2-hour time resolution during the 2018 and 2019 field campaigns. In addition, the

108   system was operated remotely following the 2018 campaign (through September 15th) to collect

109   background values at the beginning of autumn. Air was pulled continuously from an inlet on a 4

110   m meteorological tower located approximately 30 m from the instrument shelter (Van Dam et al.,

111   2013). Air passed through a sodium thiosulfate-coated O_3 scrubber for selective O_3 removal – to

112   prevent sampling losses and artifacts for reactive BVOCs (Helmig, 1997; Pollmann et al., 2005) –

113   and through a moisture trap to dry the air to a dew point of -45°C. The moisture trap was a U-

114   shaped SilcoSteel[TM] tube (stainless steel treated) cooled using thermoelectric coolers. Analytes

115   were concentrated on a Peltier-cooled (-40°C) multistage micro-adsorbent trap (50 % Tenax-GR

116   and 50 % Carboxen 1016). Analysis was accomplished by thermal desorption and injection for

117   cryogen free GC using a DB-1 column (60 m × 320 μm × 5 μm) and helium as carrier gas. The

118   oven temperature was set to 40°C for 6 minutes, then increased to 260°C at 20°C/min, and held

119   isothermally at 260°C for 13 minutes. The column flow was split between an FID and a MS for

120 simultaneous quantification and identification. Blanks and calibration standards were regularly

121 injected from a manifold. Isoprene (m/z 67 and 68), methacrolein (MACR) and methylvinylketone

122 (MVK) (m/z 41, 55, and 70), MT (m/z 68, 93, 121, and 136), and SQT (m/z 204, 91, 93, 119, and

123 69) were identified and quantified using the MS in selected ion-monitoring mode (SIM). The

124 response to isoprene was calibrated using a primary gas standard supplied by the National Physical

125 Laboratory (NPL), certified as containing 4.01±0.09 ppb of isoprene in a nitrogen matrix. The

126 analytical uncertainty for isoprene was estimated at 16 % based on the certified uncertainty of the

127 standard and on the repeatability of standard analysis throughout the campaigns. Instrument

128 responses for MACR, MVK, α-pinene, and acetonitrile were calibrated with multi-component

129 standards containing 1007 ppb MACR, 971 ppb MVK, 967 ppb α-pinene, and 1016 ppb

130 acetonitrile (Apel-Riemer Environmental Inc., Miami, FL, USA) dynamically diluted into a stream

131 of ultra-zero grade air to ~3 ppb. Quantification of other terpenoid compounds was based on GC

132 peak area (FID response) plus relative response factors using the effective carbon number concept

133 (Faiola et al., 2012; Scanlon and Willis, 1985). The limit of quantification (LOQ) was ~2 pptv

134 (pmol/mol by volume). In order to monitor and correct for long-term trends in the detection system,

135 including detector drift and decreasing performance of the adsorbent trap, we used peak areas for

136 long-lived chlorofluorocarbons (CFCs) that were monitored in the air samples together with the

137 BVOCs as an internal reference standard. The atmospheric trace gases CCl_3F (CFC-11) and

138 $CCl_2FCCl_2F_2$ (CFC-113) are ideal in this regard because they are ubiquitous in the atmosphere and

139 exhibit little spatial and temporal variability (Karbiwnyk et al., 2003; Wang et al., 2000).

140   2.2.2   Proton-Transfer-Reaction Time-of-Flight Mass-Spectrometry (PTR-ToF-MS)

141 During the summer 2019 campaign, isoprene mixing ratios in ambient air were also measured by

142 PTR-ToF-MS (model 4000, Ionicon Analytik GmbH, Innsbruck, Austria). The sample inlet was

143 located on the 4 m meteorological tower, right next to the GC-MS/FID inlet. In brief, ambient air

144 was continuously pulled through the PTR-ToF-MS drift-tube, where VOCs with proton affinities

145 higher than that of water (>165.2 kcal/mol) were ionized via proton-transfer reaction with primary

146 H_3O^+ ions, then subsequently separated and detected by a time-of-flight mass spectrometer (with

147 a mass resolving power up to 4000). At TFS, the PTR-ToF-MS measured ions from 17–400 m/z

148 every 2 minutes. Ambient air was drawn to the instrument at 10–15 L/min via ~30 m of 1/4" O.D.

149 PFA tubing maintained at ~55°C, and then subsampled by the instrument through ~100 cm of

150 1/16" O.D. PEEK tubing maintained at 60°C. The residence time from the inlet on the 4 m

151 meteorological tower to the drift-tube was less than 5 seconds. Instrument backgrounds were

152 quantified approximately every 5 hours for 20 minutes during the campaign by measuring VOC-

153 free air generated by passing ambient air through a heated catalytic converter (375 °C, platinum

154 bead, 1 % wt. Pt, Sigma Aldrich). Calibrations were typically performed every 4 days via dynamic

155 dilution of certified gas standard mixtures containing 25 distinct VOCs including isoprene (Apel-

156 Riemer Environmental Inc., Miami, FL, USA). Here, we report isoprene mixing ratios to inter-

157 compare with GC-MS measurements; other species will be reported in future work. The

158 measurement uncertainty for isoprene is ~25%, which includes uncertainties in the gas standards,

159 calibration method, and data processing.

160   2.2.3   Instrument inter-comparison

161 Figure S.I.2 shows a comparison of the GC-MS and PTR-ToF-MS isoprene mixing ratios in

162 ambient air. With a correlation coefficient of 0.93 and a linear regression slope of 0.7-1.0, the two

163 measurements agreed within their combined measurement uncertainties, in line with earlier inter-

164 comparison studies (e.g., Dunne et al., 2018; de Gouw et al., 2003). Similarly, we found a

165 correlation coefficient of 0.96 between GC-MS and PTR-ToF-MS MVK+MACR mixing ratios

166 (not shown). The good agreement between these two independent techniques gives us confidence

167 that the ambient air results presented here are robust.

168   **2.3 Ambient air vertical profiles**

169 Vertical isoprene mixing ratio profiles were obtained using a 12-foot diameter SkyDoc tethered

170 balloon. A total of eight vertical profiles were performed at ~3-hour intervals between 12:30 pm

171 Alaska Standard Time (AST) on June 15, 2019 and 11:00 am AST on June 16, 2019 in order to

172 capture a full diurnal cycle (solar noon around 2 pm AST). Sampling packages were connected to

173 the tether line such that resulting sampling heights were ~30, ~100, ~170, and ~240 m above

174 ground level. One identical sampling package was deployed at the surface. Each sampling package

175 contained an adsorbent cartridge for sample collection (see below) connected to a downstream

176 battery-powered SKC pocket pump controlled using a mechanical relay, a programmable Arduino,

177 and a real-time Clock. Once the balloon reached its apex (~ 250-300 m a.g.l.), the five pumps were

178 activated simultaneously and samples collected for 30 minutes. At the end of the 30-min sampling

179 period, the balloon was brought back down. The adsorbent cartridges were prepared in house using

180 glass tubing (89 mm long × 6.4 mm outer diameter, 4.8 mm inner diameter), and loaded with

181 Tenax-GR and Carboxen 1016 adsorbents (270 mg of each), following established practice (Ortega

182 and Helmig, 2008 and references therein). An inlet ozone scrubber was installed on each cartridge

183 to prevent BVOC sampling losses. Field blanks were collected by opening a cartridge (with no

184 pumped airflow) during each balloon flight. Following collection, adsorbent cartridges were sealed

185 with Teflon-coated brass caps and stored in the dark at ~4°C until chemical analysis. Samples were

186 analyzed at the University of Colorado Boulder following the method described in S.I. Section 1.

187 Our previous inter-comparison of this cartridge-GC-MS/FID method with independent and

188 concurrent PTR-MS observations showed that the two measurements agree to within their

189 combined uncertainties at ~25% (Hu et al., 2015). Meteorological conditions were monitored and

190 recorded during each balloon flight with a radiosonde (Met1, Grant Pass, OR, USA) attached to

191 the tethered line just below the balloon.

192 **2.4 BVOC emission rates**

193 2.4.1 Dynamic enclosure measurements

194 We used dynamic enclosure systems operated at low residence time to quantify vegetative BVOC

195 emissions following the procedure described by Ortega et al. (2008) and Ortega and Helmig

196 (2008). Two types of enclosures were used: branch and surface chambers. For branch enclosures,

197 a Tedlar® bag (Jensen Inert Products, Coral Springs, FL) was sealed around the trunk side of a

198 branch. For surface enclosures, the bag was placed around a circular Teflon® base (25 cm wide ×

199 16 cm height; see Fig. 2). For both branch and surface enclosures, the bag was connected to a

200 purge-air line and a sampling line, and positioned around the vegetation minimizing contact with

201 foliage. While purging the enclosure (see Section 2.4.3), the vegetation was allowed to acclimate

202 for 24 hours before BVOC sampling began. Samples were collected from the enclosure air,

203 concentrated onto solid-adsorbent cartridges (see Section 2.3) with an automated sampler, and

204 analyzed in-laboratory at the University of Colorado Boulder following the campaign (see S.I.

205 Section 1). Temperature and relative humidity were recorded inside and outside the enclosure (see

206 Fig. 2; S-THB-M002 sensors, Onset HOBO, Bourne, MA, USA) with a data logger (H21-USB,

207 Onset HOBO, Bourne, MA, USA). Additionally, photosynthetically active radiation (400-700 nm;

208 S-LIA-M003, Onset HOBO, Bourne, MA, USA) was measured inside the enclosure. Once

209 installed, enclosures were operated for 2-10 days. The tundra vegetation around TFS is

210 heterogeneous but most dominant species (except *Rubus chamaemorus*) were sampled. Table 1
211 presents the median relative percent cover of plant species in LTER experimental control plots at
212 TFS (Gough, 2019) and indicates whether plant species were present in surface or bag enclosures.
213 The complete list of species sampled and pictures of the enclosures are available in Figures S.I.3-
214 S.I.15; the two sampling sectors are highlighted in Fig.S.I.1. Surface enclosures were divided into
215 three vegetation types: *Salix* spp. (high isoprene emitter), *Betula* spp. (e.g., *Betula nana*
216 dominance), and miscellaneous (mix of different species, including lichens and mosses).

2.4.2 Emission rates

218 The emission rate (ER in µgC/m^2/h) for surface enclosures was calculated as follows:

219
$$ER_{surface} = \frac{(C_{out} - C_{in})Q}{S}, \qquad (1)$$

220 where C_{in} and C_{out} are the inlet and outlet analyte concentrations (in µgC/L), Q is the purge air
221 flow rate (in L/h), and S the surface area of the enclosure (in m^2).

222 The ER for branch enclosures (in µgC/g/h) was calculated as follows:

223
$$ER_{branch} = \frac{(C_{out} - C_{in})Q}{m_{dry}}, \qquad (2)$$

224 where m_{dry} is the dried mass (in g) of leaves enclosed, determined by drying the leaves – harvested
225 after the experiment – at 60-70°C until a consistent weight was achieved (Ortega and Helmig,
226 2008).

227 Emission rates were standardized to 30°C and to a PAR level of 1000 µmol/m^2/s using the
228 algorithms described in Guenther et al. (1993, 1995).

2.4.3 Enclosure purge air

230 Purge air was provided by an upstream high-capacity oil-free pump providing positive pressure to
231 the enclosure, and equipped with an in-line O$_3$ scrubber to avoid loss of reactive BVOCs from
232 reaction with O$_3$ in the enclosure air and during sampling (Helmig, 1997; Pollmann et al., 2005).
233 The purge flow was set to 25 L/min and regularly checked using a volumetric flow meter (Mesa
234 Labs Bios DryCal Defender, Butler, NJ, USA). Excess air escaped from the open end (tied around
235 the Teflon® base) while the sample air flow was pulled into the sampling line (see below).

2.4.4 Sample collection

A continuous airflow of 400-500 mL/min was drawn from the enclosure through the sampling line. A fraction of this flow was periodically collected at 265-275 mL/min on adsorbent cartridges (see Section 2.3) using a 10-cartridge autosampler (Helmig et al., 2004). During sampling, cartridges were kept at 40°C, *i.e.,* above ambient temperature, to prevent water accumulation on the adsorbent bed (Karbiwnyk et al., 2002). Samples were periodically collected in series to verify lack of analyte breakthrough. Time-integrated samples were collected for 120 min every 2 hours to establish diurnal cycles of BVOC emission. Upon collection, samples were stored in the dark at ~4°C until chemical analysis back at the University of Colorado Boulder.

2.4.5 Internal standards

In order to identify potential BVOC losses during transport, storage, and chemical analysis, 255 of the employed cartridges were pre-loaded with a four-compound standard mixture prior to the field campaigns. These internal standard compounds (toluene, 1, 2, 3-trimethylbenzene, 1, 2, 3, 4-tetrahydronaphtalene, and 1, 3, 5-triisopropylbenzene) were carefully chosen to span a wide range of volatility (C_7-C_{15}) and to not interfere (*i.e.,* coelute) with targeted BVOCs. The recovery of these four compounds was assessed at the end of the campaign, following the analytical procedure described in S.I. Section 1. Recovery rates were 101.8 ± 13.5 % (toluene), 95.2 ± 20.1 % (1,2,3-trimethylbenzene), 95.6 ± 26.6 % (1,2,3,4-tetrahydronaphtalene), and 100.9 ± 18.7 % (1,3,5-triisopropylbenzene). These results indicate that, overall, BVOC losses during transport, storage, and chemical analysis were negligible. Ortega et al. (2008) previously evaluated systematic losses of analytes to enclosure systems similar to those used here. The same four-component standard was introduced into the purge air flow of the enclosures to quantify losses as a function of volatility. That work found median losses of MT and SQT on the order of 20-30%. The emission rates presented here are therefore possibly biased low by a similar amount.

2.5 Peak fitting algorithm

The analysis of ambient air and enclosure chromatograms was performed using the TERN (Thermal desorption aerosol GC ExploreR and iNtegration package) peak fitting tool implemented in Igor Pro and available online at https://sites.google.com/site/terninigor/ (Isaacman-VanWertz et al., 2017).

2.6 Ancillary parameters

Meteorological parameters. A suite of meteorological instruments was deployed on the 4 m tower. Wind speed and direction were measured at ~4 m above ground level with a Met One 034B-L sensor. As described by Van Dam et al. (2013), temperature was measured at three different heights using RTD temperature probes (model 41342, R.M. Young Company, Traverse City, MI) housed in aspirated radiation shields (model 43502, R.M. Young Company, Traverse City, MI). Regular same-height inter-comparisons were conducted to test for instrumental offsets. Incoming and reflected solar radiation were recorded with LI200X pyranometers (Campbell Scientific Instruments).

In addition, historical (1988-2019) meteorological data recorded by TFS Environmental Data Center are available at: https://toolik.alaska.edu/edc/abiotic_monitoring/data_query.php

Particle measurements. A Met One Instruments Model 212-2 8-channel (0.3 to 10 µm) particle profiler was operated continuously on the roof of the weatherproof instrument shelter. This instrument uses a laser-diode based optical sensor and light scatter technology to detect, size, and count particles (http://mail.metone.com/particulate-Aero212.htm).

Nitrogen oxides. Nitrogen oxides (NO_x) were measured with a custom-built, high sensitivity (~5 pptv detection limit) single-channel chemiluminescence analyzer (Fontijn et al., 1970). The instrument monitors nitric oxide (NO) and nitrogen dioxide (NO_2) in ambient air using a photolytic converter. Automated switching valves alternated between NO and NO_2 mode every 30 minutes. Calibration was accomplished by dynamic dilution of a 1.5 ppm compressed NO gas standard (Scott-Marrin, Riverside, CA, USA).

2.7 Theoretical response of isoprene emissions to temperature in MEGAN2.1

We applied our isoprene emission measurements to evaluate the temperature response algorithms embedded in MEGAN2.1 (Guenther et al., 2012). Theoretical isoprene emission rates (F_T) were calculated for TFS as:

$$F_T = C_{CE} \, \gamma_T \, \sum_j \varkappa_j \, \varepsilon_j \qquad (3)$$

where C_{CE} is the canopy environment coefficient (assigned a value that results in $\gamma_T = 1$ under standard conditions), and ε_j is the emission factor under standard conditions for vegetation type j

293 with fractional grid box areal coverage $\varkappa_j$. We used $\sum_j \varkappa_j \, \varepsilon_j = 2766$ µg/m^2/h at TFS based on the

294 high resolution (1 km) global emission factor input file available at

295 https://bai.ess.uci.edu/megan/data-and-code/megan21. The temperature activity factor (γ_T) was

296 calculated as:

297 $\quad \gamma_T = E_{opt} \times \dfrac{200\, e^{95\,x}}{200 - 95 \times (1 - e^{200\,x})}$ $\qquad\qquad$ (4)

298 with

299 $\quad x = \dfrac{\frac{1}{T_{opt}} - \frac{1}{T}}{0.00831}$ $\qquad\qquad$ (5)

300 $\quad E_{opt} = 2 \times e^{0.08(T_{10} - 297)}$ $\qquad\qquad$ (6)

301 $\quad T_{opt} = 313 + 0.6(T_{10} - 297),$ $\qquad\qquad$ (7)

302 where T is the enclosure ambient air temperature and T_{10} the average enclosure air temperature

303 over the past 10 days.

3. Results and Discussion

3.1 Ambient air mixing ratios

3.1.1 Isoprene and oxidation products

307 Figure 3 (top panels) shows the time-series of isoprene mixing ratios in ambient air recorded over

308 the course of this study at TFS with the GC system. Mixing ratios were highly variable and ranged

309 from below the quantification limit to 505 pptv (mean of 36.1 pptv). The PTR-ToF-MS gave

310 similar results (see Fig.S.I.16a). These mixing ratios fall within the range of values reported in the

311 Eurasian taiga (e.g., Hakola et al., 2000, 2003; Lappalainen et al., 2009). For example, Hakola et

312 al. (2003) reported a maximum monthly mean mixing ratio of 98 pptv (in July) in Central Finland

313 while Hakola et al. (2000) observed mixing ratios ranging from a few pptv to ~600 pptv in Eastern

314 Finland. In general, however, BVOC emissions in the Eurasian taiga are relatively low compared

315 to forest ecosystems in warmer climates and are dominated by monoterpenes (Rinne et al., 2009).

316 Isoprene mixing ratios peaked on August 1, 2018 around 4 pm and on June 20, 2019 around 10

317 pm, respectively. These two peaks occurred 3-5 hours after the daily maximum ambient

318 temperature was reached (17.8°C in 2019 and 21.8°C in 2019 – see Fig. 3). The isoprene peak on

319   June 20, 2019 was concomittant with enhanced acetonitrile mixing ratios and particle counts (see
320   Fig. 4), reflecting unusually hazy conditions that day at TFS. We attribute the particle and
321   acetonitrile enhancements to intense wildfires occurring across the Arctic Circle at that time – most
322   of them in southern Alaska and Siberia (Earth Observatory, 2019). Acetonitrile increased by a
323   factor of 4 during this event, compared to a factor of 21 increase for isoprene. The higher emission
324   factor for acetonitrile *vs.* isoprene from biomass burning in boreal forests (Akagi et al., 2011) and
325   the relatively short lifetime of isoprene (Atkinson, 2000) indicate that the observed isoprene
326   enhancement was due to fresh local biogenic emissions rather than transported wildfire emissions.

327   Over the course of this study, we recorded MACR and MVK mixing ratios respectively ranging
328   from below the quantification limit to 95 pptv (12.4 ± 16.1 pptv; mean ± standard deviation) and
329   from below the quantification limit to 450 pptv (43.1 ± 66.7 pptv; see Fig. 3, top panels). The PTR-
330   ToF-MS gave similar results (see Fig.S.I.16b). Median NO and NO_2 mixing ratios of 21 and 74
331   pptv, respectively, during the 2019 campaign (not shown) suggest a low-NO_x environment, in line
332   with previous studies at several Arctic locations (Bakwin et al., 1992; Honrath and Jaffe, 1992).
333   Under such conditions, MACR and MVK mixing ratios should be used as upper estimates as it has
334   been noted that some low-NO_x isoprene oxidation products (isoprene hydroxyhydroperoxides) can
335   undergo rearragement in GC and PTR-MS instruments and be misidentified as MACR and MVK
336   (Rivera-Rios et al., 2014). We found a high correlation between MACR and MVK ($R^2 = 0.95$, p <
337   0.01) and between these two compounds and isoprene ($R^2 \sim 0.80$, p < 0.01). Increases of MACR
338   and MVK mixing ratios above the background were mostly concomitant with isoprene increases,
339   suggesting that atmospheric or within-plant oxidation of isoprene was their main source
340   (Biesenthal et al., 1997; Hakola et al., 2003; Jardine et al., 2012). The mean ratio of MVK to
341   MACR was 2.7, within the range reported by earlier studies (e.g., Apel et al., 2002; Biesenthal and
342   Shepson, 1997; Hakola et al., 2003; Helmig et al., 1998), and no clear diurnal cycle in the ratio
343   was found. This record of ambient air isoprene, MACR, and MVK mixing ratios is, to the best of
344   our knowledge, the first in an Arctic tundra environment. The combined measurement of isoprene
345   and its oxidation products provides a new set of observations to further constrain isoprene
346   chemistry under low-NO_x conditions in atmospheric models (e.g., Bates and Jacob, 2019).

347   3.1.2   Isoprene vertical profiles

348   Figure 5 shows vertical profiles (0 to ~250 m a.g.l.) of isoprene mixing ratios derived from the 30-

349   min tethered balloon samples collected on June 15 and 16, 2019. Temperature profiles (see

350   Fig.S.I.17) indicate that most of the flights were performed in a convective boundary layer (Holton

351   and Hakim, 2013). A nocturnal boundary layer was, however, observed in the first ~50 m from ~2

352   am to ~4:30 am (see Fig.S.I.17e-f) – with temperature increasing with elevation.

353   Except during the last flight, isoprene mixing ratios were in the range of background levels (~0-

354   50 pptv) reported with the GC-MS (see Section 3.1.1). Samples collected from 10-10:30 am on

355   June 16 (see Fig. 5h) showed a pronounced gradient, with 200 pptv at ground level and decreasing

356   mixing ratios with elevation. This maximum at ground-level is expected for a VOC with a surface

357   source (Helmig et al., 1998) while the 200 pptv mixing ratio can likely be attributed to a

358   temperature-driven increase of isoprene emissions by the surrounding vegetation. Indeed, the

359   ambient temperature at ground-level was higher during that flight than during the previous ones

360   (see Fig.S.I.17h). The diurnal cycles of isoprene emissions and temperature are further discussed

361   in Section 3.2.2. Interestingly, the GC-MS and the PTR-ToF-MS did not capture this 200 pptv

362   maximum (see Fig. 3 and Fig.S.I.16), which may be because the balloon flights were performed

363   at a different location (near sampling sector B, see Fig.S.I.1) surrounded by a higher fraction of

364   isoprene-emitting shrubs (willow).

365   Samples collected on June 16, 2019 from 4 to 4:30 am (see Fig. 5f) show decreasing isoprene

366   mixing ratios with increasing elevation, suggesting higher levels (25-50 pptv) in the nocturnal

367   boundary layer than above. This result suggests continuing isoprene emissions by the surrounding

368   vegetation under low-PAR conditions. This is further discussed in Section 3.2.2.

369   3.1.3   Monoterpenes and Sesquiterpenes

370   MT mixing ratios ranged from 3 to 537 pptv (14 ± 18 pptv; median ± standard deviation) during

371   the 2019 campaign according to the PTR-ToF-MS measurements. Using the GC-MS/FID, we were

372   able to detect and quantify the following MT in ambient air: α-pinene, camphene, sabinene, p-

373   cymene, and limonene. Mean mixing ratios are reported in Table 2 (for values lower than the LOQ,

374   mixing ratios equal to half of the LOQ are used). These compounds have been previously identified

375   as emissions of the widespread circumpolar dwarf birch *Betula nana* (Li et al., 2019; Vedel-

376   Petersen et al., 2015) and other high Arctic vegetation (Schollert et al., 2014). The quantification

377   frequency of camphene, sabinene, p-cymene, and limonene was low (see Table 2) and MT mixing

378 ratios in ambient air were dominated by α-pinene. Several prior studies performed at boreal sites
379 have similarly identified α-pinene as the most abundant monoterpene throughout the growing
380 season (e.g., Hakola et al., 2000; Lindfors et al., 2000; Spirig et al., 2004; Tarvainen et al., 2007).
381 We did not detect any sesquiterpene in ambient air above the 2 pptv instrumental LOQ.

382 Overall, isoprene and α-pinene dominated the ambient air BVOC profile at TFS, respectively
383 constituting ~72% and ~24% of total BVOCs quantified in ambient air (on a mixing-ratio basis).

384 **3.2 Emission rates**

385 3.2.1 Branch enclosures

386 A branch enclosure experiment was performed from July 27 to August 2, 2018 on *Salix glauca* to
387 investigate BVOC emission rates per dry weight plant biomass (see Fig.S.I.5). Isoprene emission
388 rates ranged from <0.01 to 11 µgC/g/h (with a mean enclosure temperature of 16.5°C and mean
389 PAR of 880 µmol/m^2/s), in line with non-normalized emission rates reported at Kobbefjord,
390 Greenland by Kramshøj et al. (2016; Supplementary Table 5) for the same species under slightly
391 different environmental conditions (mean temperature of 24.6°C and mean PAR of 1052
392 µmol/m^2/s). Once standardized to 30°C and 1000 µmol/m^2/s, our emission rates averaged 5
393 µgC/g/h, in good agreement with standardized emissions reported at Kobbefjord (mean of 7
394 µgC/g/h) by Vedel-Petersen et al. (2015). The quantified MTs had emissions averaging two orders
395 of magnitude lower than those of isoprene (0.01 vs 1 µgC/g/h). Emission rates for the sum of α-
396 pinene, β-pinene, limonene, camphene, and 1,8-cineole ranged from <0.01 to 0.06 µgC/g/h. These
397 results are again in good agreement with those reported for the same species at Kobbefjord (~0.01
398 µgC/g/h) by Kramshøj et al. (2016; Supplementary Table 5).

399 3.2.2 Surface emission rates

400 The isoprene surface emission rate, as inferred from surface enclosures, was highly variable and
401 ranged from 0.2 to ~2250 µgC/m^2/h (see Fig. 6). The 2250 µgC/m^2/h maximum, reached on June
402 26, 2019, with an enclosure temperature of 32°C, is higher than maximum values reported at TFS
403 by Potosnak et al. (2013) (1200 µgC/m^2/h at an air temperature of 22°C). It should be noted that
404 these maximum values were observed at different ambient temperatures; we further investigate the
405 temperature dependency of isoprene emissions in Section 3.3. Elevated surface emission rates (*i.e.,*
406 > 500 µgC/m^2/h) were all observed while sampling enclosures dominated by *Salix* spp.. At TFS,

14

407   the overall 24-hour mean isoprene emission rate amounted to 85 µgC/m^2/h, while the daytime (10

408   am-8 pm) and midday (11 am-2 pm) means were 140 and 213 µgC/m^2/h, respectively. To put this

409   in perspective, the average isoprene surface emission rate standardized to 30°C and 1000

410   µmol/m^2/s (~ 300 µgC/m^2/h) was an order of magnitude lower than emission rates reported for

411   warmer mid-latitude or tropical forests. For example, average midday fluxes of 3000 µgC/m^2/h

412   were reported in a northern hardwood forest in Michigan (Pressley et al., 2005), while several

413   reports of isoprene emissions from tropical ecosystems give daily estimates of 2500-3000

414   µgC/m^2/h (Helmig et al., 1998; Karl et al., 2004; Rinne et al., 2002).

415   Figure 7 shows the measured surface emission rates for α-pinene, β-pinene, limonene, and 1,8-

416   cineole. While p-cymene, sabinene, 3-carene, and isocaryophyllene (SQT) were detected in some

417   of the surface enclosure samples, we focus the discussion on the most frequently quantified

418   compounds. It is worth noting that the most frequently observed compounds in enclosure samples

419   are among the most frequently seen MT in ambient air (see Section 3.1.3). Regardless of the

420   species, emission rates remained on average below 1 µgC/m^2/h over the course of the study (see

421   Table 3). These results are at the low end of emission rates reported for four vegetation types in

422   high Arctic Greenland (Schollert et al., 2014), but in line with results reported at Kobbefjord,

423   Greenland by Kramshøj et al. (2016; Supplementary Table 4).

424   Figures 8a-c show the mean diurnal cycle (over the two campaigns) of isoprene surface emission

425   rates for different vegetation types (see Fig.S.I.3-15 for nomenclature). The two field campaigns

426   were carried out during the midnight sun period, which could possibly sustain BVOC emissions

427   during nighttime. It should, however, be noted that low sun angles translate to very low PAR and

428   a typical diurnal pattern is observed in summer at TFS despite 24 hours of light (see Fig. 8h).

429   Regardless of the vegetation type, isoprene emission rates exhibited a significant diurnal cycle

430   with an early afternoon maximum, in line with the mean diurnal cycle of enclosure temperature

431   and PAR. These results are in line with the well-established diurnal variation of BVOC emissions

432   in environments ranging from Mediterranean to boreal forests (e.g., Fares et al., 2013; Liu et al.,

433   2004; Ruuskanen et al., 2005; Zini et al., 2001) and with the correlation between isoprene ambient

434   air mixing ratios and temperature at TFS (see Section 3.1). Despite the relatively low MT emission

435   rates, a significant diurnal cycle was also observed with peak total MT emissions of ~1 µgC/m^2/h

436   during early afternoon for both *Salix* spp. and *Betula* spp. (Fig. 8e-f). A summary of emission rates

per vegetation type and time of day is given in Table 3. As can be seen in Table 3 and Fig. 8, PAR and BVOC emissions significantly decreased at night but were still detectable. These sustained BVOC emissions during nighttime confirm observations by Lindwall et al. (2015) during a 24-hour experiment with five different Arctic vegetation communities and explain the higher isoprene levels observed in the nocturnal boundary layer than above during the diurnal balloon experiment (see Section 3.1.2).

The ratio of total MT (given by the sum of α-pinene, β-pinene, limonene, and 1,8-cineole) emissions to isoprene emissions was an order of magnitude higher for *Betula* spp. (0.22) than for *Salix* spp. (0.03). This result, driven by the relatively lower isoprene emissions of *Betula* spp., is in line with earlier studies, suggesting similar emission characteristics for Arctic plants (e.g., Kramshøj et al., 2016; Vedel-Petersen et al., 2015).

4. Insights into future changes

4.1 Response of isoprene emissions to temperature

The Arctic has warmed significantly during the last three decades and temperatures are projected to increase an additional 5-13°C by the end of the century (Overland et al., 2014). Heat wave frequency is also increasing in the terrestrial Arctic (Dobricic et al., 2020). For example, western Siberia experienced an unusually warm May in 2020, with temperatures of 20-25°C (Freedman and Cappucci, 2020). In that context, numerous studies have pointed out the likelihood of increased BVOC emissions due to Arctic warming and associated vegetation and land cover change (Faubert et al., 2010; Potosnak et al., 2013; Rinnan et al., 2011; Tiiva et al., 2008).

Over the course of the two field campaigns at TFS, BVOC surface emission rates were measured over a large span of enclosure temperatures (2-41°C). While isoprene and MT emissions respond to leaf temperature (Guenther et al., 1993), air temperature was used here in place of leaf temperature – which has been assumed before in the literature for high-latitude ecosystems (e.g., Olofsson et al., 2005; Potosnak et al., 2013). Several studies have, however, suggested a decoupling of leaf and air temperature in tundra environments (Lindwall et al., 2016; Potosnak et al., 2013). With predicted increase of air temperature in the Arctic, it still remains largely unknown how leaf temperature will change and impact BVOC emissions. As suggested by Tang et al. (2016), long-term parallel observations of both leaf and air temperature are needed. The response

466 of BVOC emissions to temperature discussed here should be interpreted with this potential caveat
467 in mind.

468 While MT emissions remained low and close to the detection limit thus preventing robust
469 quantification of any emission-temperature relationship, isoprene emissions significantly
470 increased with temperature (Fig.9). Figure 9 combines daytime (e.g., with relatively high PAR
471 values) isoprene emission rates from different surface enclosures, with results normalized to
472 account for differing total biomass and species distributions (with *Salix* spp. the dominant emitter).
473 Specifically, we divided all fluxes by the enclosure-specific mean emission at $20 \pm 1°C$. Emission
474 rates are often standardized to 30°C but we employ 20°C here owing to the colder growth
475 environment at TFS (Ekberg et al., 2009). The isoprene emission-temperature relationship
476 observed at TFS (in blue) is very similar to that reported by Tang et al. (2016) at Abisko (Sweden;
477 in pink) for tundra heath (dominated by evergreen and deciduous dwarf shrubs). Results at TFS
478 and Abisko both point to a high isoprene-temperature response for Arctic ecosystems (Tang et al.,
479 2016). This is further supported by two warming experiments performed in mesic tundra heath
480 (dominated by *Betula nana*, *Empetrum nigrum*, *Empetrum hermaphroditum*, and *Cassiope*
481 *tetragona*) and dry dwarf-shrub tundra (co-dominated by *Empetrum hermaphroditum* and *Salix*
482 *glauca*) in Western Greenland (Kramshøj et al., 2016; Lindwall et al., 2016). Kramshøj et al.
483 (2016) observed a 240% isoprene emission increase with 3°C warming, while Lindwall et al.
484 (2016) reported a 280% increase with 4°C warming. The observationally-derived emission-
485 temperature relationship derived here for TFS reveals a 180-215% emission increase with 3-4°C
486 warming.

487 The MEGAN2.1 modeling framework is commonly used to estimate BVOC fluxes between
488 terrestrial ecosystems and the atmosphere (e.g., Millet et al., 2018). Here, we apply the TFS
489 observations to evaluate the MEGAN2.1 emission-temperature relationship for this Arctic
490 environment. Figure 9 shows that the model temperature algorithm provides a close fit with
491 observations below 30°C, with a 170-240% emission increase for a 3-4°C warming. While the
492 model predicts a leveling-off of emissions at approximately 30-35°C, our observations reveal no
493 such phenomenon within the 0-40°C enclosure temperature range (Fig. 9). However, given the
494 limited number of enclosure measurements above 30°C, a leveling-off of emissions cannot be
495 statistically ruled out. The key result here is that MEGAN2.1 adequately reproduces the

17

496   temperature dependence response of Arctic ecosystems in the 0-30°C temperature range – ambient

497   temperature > 30°C being unlikely. The highest air temperature on record at TFS (1988-2019) is

498   26.5°C, and the mean summertime (June-August) temperature over that period is 9°C.

499   Additionally, for each year in the 1988-2019 historical dataset, there were only 1 to 23 days (0 to

500   4 days) per year with a maximum temperature above 20°C (above 25°C). If global greenhouse gas

501   emissions continue to increase, temperatures are expected to rise 6-7°C in northern Alaska by the

502   end of the century (annual average; Markon et al., 2012) while the number of days with

503   temperatures above 25°C could triple (Lader et al., 2017). Based on current climate conditions and

504   this rate of change, the MEGAN2.1 algorithm adequately represents the temperature dependence

505   response of Arctic ecosystems for the near and intermediate-term future.

506   4.2 Long-term effects of warming

507   BVOC produced by plants are involved in plant growth, reproduction, and defense, and plants use

508   isoprene emissions as a thermotolerance mechanism (Peñuelas and Staudt, 2010; Sasaki et al.,

509   2007). The exponential response of isoprene emissions to temperature observed at TFS adds to a

510   growing body of evidence indicating a high isoprene-temperature response in Arctic ecosystems.

511   However, observations at TFS do not necessarily reflect long-term effects of warming. Schollert

512   et al., (2015) examined how long-term warming affects leaf anatomy of individual arctic plant

513   shoots (*Betula nana*, *Cassiope tetragona*, *Empetrum hermaphroditum*, and *Salix arctica*). They

514   found that long-term warming results in significantly thicker leaves suggesting anatomical

515   acclimation. While the authors hypothesized that this anatomical acclimation may limit the

516   increase of BVOC emissions at plant shoot-level, Kramshøj et al. (2016) later showed that BVOC

517   emissions from Arctic tundra exposed to six years of experimental warming increase at both the

518   plant shoot and ecosystem levels.

519   In addition to the direct impact of long-term warming on BVOC emissions, ecosystem-level

520   emissions are expected to increase in the Arctic due to climate-driven changes in plant biomass

521   and vegetation composition. For instance, the widespread increase in shrub abundance in the Arctic

522   – due to a longer growing season and enhanced nutrient availability (Berner et al., 2018; Sturm et

523   al., 2001) – will likely significantly affect the BVOC emission potential of the Arctic tundra.

524   Additionally, as mentioned above and as discussed extensively by Peñuelas and Staudt (2010) and

525   Loreto and Schnitlzer (2010), emissions of BVOCs might be largely beneficial for plants,

526　conferring them higher protection from abiotic stressors which are predicted to be more severe in

527　the future. Long-term arctic warming may thus favor BVOC-emitting species even further.

528　**5. Conclusion**

529　While BVOC ambient concentrations and emission rates have been frequently measured in boreal

530　ecosystems, Arctic tundra environments are under studied. We provide here summertime BVOC

531　ambient air mixing ratios and emission rates at Toolik Field Station, on the north flank of the

532　Brooks Range in northern Alaska. We present the first continuous summertime record of ambient

533　air isoprene and its first-generation oxidation products in the Arctic tundra environment. This

534　dataset provides a new set of observations to constrain isoprene chemistry in low-NO_x

535　environments. This dataset also provides a baseline to investigate future changes in the BVOC

536　emission potential of the Arctic tundra environment. While the overall mean isoprene emission

537　rate amounted to 85 $\mu gC/m^2/h$, elevated (> 500 $\mu gC/m^2/h$) isoprene surface emission rates were

538　observed for *Salix* spp., a known isoprene emitter. We also show that the reponse to temperature

539　of isoprene emissions in enclosures dominated by *Salix* spp. increased exponentially in the 0-40°C

540　range, likely conferring greater thermal protection for these plants. Given the widespread increase

541　in shrub abundance in the Arctic (including *Salix* spp.), our results support earlier studies (e.g.,

542　Valolahti et al., 2015) suggesting that climate-induced changes in the Arctic vegetation

543　composition will significantly affect the BVOC emission potential of the Arctic tundra, with

544　implications for atmospheric oxidation processes and climate feedbacks.

545　**Data availability**

546　Data are available upon request to the corresponding author.

547　**Author contribution**

548　DH, LH, and DBM designed the experiments and acquired funding. HA led the two field

549　campaigns with significant on-site contribution from KM, JH, LH, DBM, KC, JM, CW, TM, and

550　DH. JH designed and built most of the instruments used in this study. CW acquired the PTR-ToF-

551　MS data during the second campaign and DK performed data analysis. MSBH identified the plant

552　species and provided guidance during the field campaigns. KM and HA analyzed the samples in

553　the lab. HA analyzed all the data and prepared the manuscript with contributions from all co-

554　authors.

Competing interests

The authors declare no competing interests.

Acknowledgements

References

Akagi, S. K., Yokelson, R. J., Wiedinmyer, C., Alvarado, M. J., Reid, J. S., Karl, T., Crounse, J. D. and Wennberg, P. O.: Emission factors for open and domestic biomass burning for use in atmospheric models, Atmospheric Chem. Phys., 11(9), 4039–4072, doi:https://doi.org/10.5194/acp-11-4039-2011, 2011.

Apel, E. C., Riemer, D. D., Hills, A., Baugh, W., Orlando, J., Faloona, I., Tan, D., Brune, W., Lamb, B., Westberg, H., Carroll, M. A., Thornberry, T. and Geron, C. D.: Measurement and interpretation of isoprene fluxes and isoprene, methacrolein, and methyl vinyl ketone mixing ratios at the PROPHET site during the 1998 Intensive, J. Geophys. Res. Atmospheres, 107(D3), ACH 7-1-ACH 7-15, doi:10.1029/2000JD000225, 2002.

Arneth, A., Harrison, S. P., Zaehle, S., Tsigaridis, K., Menon, S., Bartlein, P. J., Feichter, J., Korhola, A., Kulmala, M., O'Donnell, D., Schurgers, G., Sorvari, S. and Vesala, T.: Terrestrial biogeochemical feedbacks in the climate system, Nat. Geosci., 3(8), 525–532, doi:10.1038/ngeo905, 2010.

Atkinson, R.: Atmospheric chemistry of VOCs and NOx, Atmos. Environ., 34(12), 2063–2101, doi:10.1016/S1352-2310(99)00460-4, 2000.

Bakwin, P. S., Wofsy, S. C., Fan, S.-M. and Fitzjarrald, D. R.: Measurements of NO x and NO y concentrations and fluxes over Arctic tundra, J. Geophys. Res. Atmospheres, 97(D15), 16545–16557, doi:10.1029/91JD00929, 1992.

Bates, K. H. and Jacob, D. J.: A new model mechanism for atmospheric oxidation of isoprene: global effects on oxidants, nitrogen oxides, organic products, and secondary organic aerosol, Atmospheric Chem. Phys., 19(14), 9613–9640, doi:https://doi.org/10.5194/acp-19-9613-2019, 2019.

Berner, L. T., Jantz, P., Tape, K. D. and Goetz, S. J.: Tundra plant above-ground biomass and shrub dominance mapped across the North Slope of Alaska, Environ. Res. Lett., 13(3), 035002, doi:10.1088/1748-9326/aaaa9a, 2018.

Biesenthal, T. A. and Shepson, P. B.: Observations of anthropogenic inputs of the isoprene oxidation products methyl vinyl ketone and methacrolein to the atmosphere, Geophys. Res. Lett., 24(11), 1375–1378, doi:10.1029/97GL01337, 1997.

Biesenthal, T. A., Wu, Q., Shepson, P. B., Wiebe, H. A., Anlauf, K. G. and Mackay, G. I.: A study of relationships between isoprene, its oxidation products, and ozone, in the Lower Fraser Valley, BC - ScienceDirect, Atmospheric Environment, 31(14), 2049–2058, 1997.

Carlton, A. G., Wiedinmyer, C. and Kroll, J. H.: A review of Secondary Organic Aerosol (SOA) formation from isoprene, Atmospheric Chem. Phys., 9(14), 4987–5005, doi:https://doi.org/10.5194/acp-9-4987-2009, 2009.

Dobricic, S., Russo, S., Pozzoli, L., Wilson, J. and Vignati, E.: Increasing occurrence of heat waves in the terrestrial Arctic, Environ. Res. Lett., 15(2), 024022, doi:10.1088/1748-9326/ab6398, 2020.

605 Dunne, E., Galbally, I. E., Cheng, M., Selleck, P., Molloy, S. B. and Lawson, S. J.: Comparison
606 of VOC measurements made by PTR-MS, adsorbent tubes–GC-FID-MS and DNPH
607 derivatization–HPLC during the Sydney Particle Study, 2012: a contribution to the assessment of
608 uncertainty in routine atmospheric VOC measurements, Atmospheric Meas. Tech., 11(1), 141–
609 159, doi:https://doi.org/10.5194/amt-11-141-2018, 2018.

610 Earth Observatory: Arctic Fires Fill the Skies with Soot, [online] Available from:
611 https://earthobservatory.nasa.gov/images/145380/arctic-fires-fill-the-skies-with-
612 soot#targetText=In%20June%20and%20July%202019,harmful%20particles%20into%20the%20
613 air. (Accessed 16 October 2019), 2019.

614 Ekberg, A., Arneth, A., Hakola, H., Hayward, S. and Holst, T.: Isoprene emission from wetland
615 sedges, Biogeosciences, 6(4), 601–613, doi:10.5194/bg-6-601-2009, 2009.

616 Ekberg, A., Arneth, A. and Holst, T.: Isoprene emission from Sphagnum species occupying
617 different growth positions above the water table, Boreal Environ. Res. Int. Interdiscip. J., 16(1),
618 47–59, 2011.

619 Elmendorf, S. C., Henry, G. H. R., Hollister, R. D., Björk, R. G., Boulanger-Lapointe, N., Cooper,
620 E. J., Cornelissen, J. H. C., Day, T. A., Dorrepaal, E., Elumeeva, T. G., Gill, M., Gould, W. A.,
621 Harte, J., Hik, D. S., Hofgaard, A., Johnson, D. R., Johnstone, J. F., Jónsdóttir, I. S., Jorgenson, J.
622 C., Klanderud, K., Klein, J. A., Koh, S., Kudo, G., Lara, M., Lévesque, E., Magnússon, B., May,
623 J. L., Mercado-Dı´az, J. A., Michelsen, A., Molau, U., Myers-Smith, I. H., Oberbauer, S. F.,
624 Onipchenko, V. G., Rixen, C., Schmidt, N. M., Shaver, G. R., Spasojevic, M. J., Þórhallsdóttir, Þ.
625 E., Tolvanen, A., Troxler, T., Tweedie, C. E., Villareal, S., Wahren, C.-H., Walker, X., Webber,
626 P. J., Welker, J. M. and Wipf, S.: Plot-scale evidence of tundra vegetation change and links to
627 recent summer warming, Nat. Clim. Change, 2(6), 453–457, doi:10.1038/nclimate1465, 2012.

628 Faiola, C. L., Erickson, M. H., Fricaud, V. L., Jobson, B. T. and VanReken, T. M.
629 (orcid:0000000226454911): Quantification of biogenic volatile organic compounds with a flame
630 ionization detector using the effective carbon number concept, Atmospheric Meas. Tech. Online,
631 5(8), doi:10.5194/amt-5-1911-2012, 2012.

632 Fares, S., Schnitzhofer, R., Jiang, X., Guenther, A., Hansel, A. and Loreto, F.: Observations of
633 Diurnal to Weekly Variations of Monoterpene-Dominated Fluxes of Volatile Organic Compounds
634 from Mediterranean Forests: Implications for Regional Modeling, Environ. Sci. Technol., 47(19),
635 11073–11082, doi:10.1021/es4022156, 2013.

636 Faubert, P., Tiiva, P., Rinnan, Å., Michelsen, A., Holopainen, J. K. and Rinnan, R.: Doubled
637 volatile organic compound emissions from subarctic tundra under simulated climate warming,
638 New Phytol., 187(1), 199–208, doi:10.1111/j.1469-8137.2010.03270.x, 2010.

639 Fehsenfeld, F., Calvert, J., Fall, R., Goldan, P., Guenther, A. B., Hewitt, C. N., Lamb, B., Liu, S.,
640 Trainer, M., Westberg, H. and Zimmerman, P.: Emissions of volatile organic compounds from
641 vegetation and the implications for atmospheric chemistry, Glob. Biogeochem. Cycles, 6(4), 389–
642 430, doi:10.1029/92GB02125, 1992.

643 Fontijn, Arthur., Sabadell, A. J. and Ronco, R. J.: Homogeneous chemiluminescent measurement
644 of nitric oxide with ozone. Implications for continuous selective monitoring of gaseous air
645 pollutants, Anal. Chem., 42(6), 575–579, doi:10.1021/ac60288a034, 1970.

646 Forbes, B. C., Fauria, M. M. and Zetterberg, P.: Russian Arctic warming and 'greening' are closely
647 tracked by tundra shrub willows, Glob. Change Biol., 16(5), 1542–1554, doi:10.1111/j.1365-
648 2486.2009.02047.x, 2010.

649 Freedman, A. and Cappucci, M.: Parts of Siberia are hotter than Washington, with temperatures
650 nearly 40 degrees above average, Wash. Post, 22nd May [online] Available from:
651 https://www.washingtonpost.com/weather/2020/05/22/siberia-heat-wave/ (Accessed 29 May
652 2020), 2020.

653 Fuentes, J. D., Lerdau, M., Atkinson, R., Baldocchi, D., Bottenheim, J. W., Ciccioli, P., Lamb, B.,
654 Geron, C., Gu, L., Guenther, A., Sharkey, T. D. and Stockwell, W.: Biogenic Hydrocarbons in the
655 Atmospheric Boundary Layer: A Review, Bull. Am. Meteorol. Soc., 81(7), 1537–1576,
656 doi:10.1175/1520-0477(2000)081<1537:BHITAB>2.3.CO;2, 2000.

657 Gough, L.: Relative percent cover of plant species for years 2012-2017 in the Arctic Long-term
658 Ecological Research (ARC-LTER) 1989 moist acidic tundra (MAT89) experimental plots, Toolik
659 Field Station, Alaska., , doi:10.6073/PASTA/F31DEF760DB3F8E6CFEE5FEE07CC693E, 2019.

660 de Gouw, J. A., Goldan, P. D., Warneke, C., Kuster, W. C., Roberts, J. M., Marchewka, M.,
661 Bertman, S. B., Pszenny, A. a. P. and Keene, W. C.: Validation of proton transfer reaction-mass
662 spectrometry (PTR-MS) measurements of gas-phase organic compounds in the atmosphere during
663 the New England Air Quality Study (NEAQS) in 2002, J. Geophys. Res. Atmospheres, 108(D21),
664 doi:10.1029/2003JD003863, 2003.

665 Guenther, A., Hewitt, C. N., Erickson, D., Fall, R., Geron, C., Graedel, T., Harley, P., Klinger, L.,
666 Lerdau, M., Mckay, W. A., Pierce, T., Scholes, B., Steinbrecher, R., Tallamraju, R., Taylor, J. and
667 Zimmerman, P.: A global model of natural volatile organic compound emissions, J. Geophys. Res.
668 Atmospheres, 100(D5), 8873–8892, doi:10.1029/94JD02950, 1995.

669 Guenther, A., Karl, T., Harley, P., Wiedinmyer, C., Palmer, P. I. and Geron, C.: Estimates of global
670 terrestrial isoprene emissions using MEGAN (Model of Emissions of Gases and Aerosols from
671 Nature), Atmospheric Chem. Phys., 6(11), 3181–3210, doi:https://doi.org/10.5194/acp-6-3181-
672 2006, 2006.

673 Guenther, A. B., Zimmerman, P. R., Harley, P. C., Monson, R. K. and Fall, R.: Isoprene and
674 monoterpene emission rate variability: Model evaluations and sensitivity analyses, J. Geophys.
675 Res. Atmospheres, 98(D7), 12609–12617, doi:10.1029/93JD00527, 1993.

676 Guenther, A. B., Jiang, X., Heald, C. L., Sakulyanontvittaya, T., Duhl, T., Emmons, L. K. and
677 Wang, X.: The Model of Emissions of Gases and Aerosols from Nature version 2.1 (MEGAN2.1):
678 an extended and updated framework for modeling biogenic emissions, Geosci. Model Dev., 5(6),
679 1471–1492, doi:https://doi.org/10.5194/gmd-5-1471-2012, 2012.

680 Hakola, H., Laurila, T., Rinne, J. and Puhto, K.: The ambient concentrations of biogenic
681 hydrocarbons at a northern European, boreal site, Atmos. Environ., 34(29), 4971–4982,
682 doi:10.1016/S1352-2310(00)00192-8, 2000.

683 Hakola, H., Tarvainen, V., Laurila, T., Hiltunen, V., Hellén, H. and Keronen, P.: Seasonal variation
684 of VOC concentrations above a boreal coniferous forest, Atmos. Environ., 37(12), 1623–1634,
685 doi:10.1016/S1352-2310(03)00014-1, 2003.

686 Helmig, D.: Ozone removal techniques in the sampling of atmospheric volatile organic trace gases,
687 Atmos. Environ., 31(21), 3635–3651, doi:10.1016/S1352-2310(97)00144-1, 1997.

688 Helmig, D., Balsley, B., Davis, K., Kuck, L. R., Jensen, M., Bognar, J., Smith, T., Arrieta, R. V.,
689 Rodríguez, R. and Birks, J. W.: Vertical profiling and determination of landscape fluxes of
690 biogenic nonmethane hydrocarbons within the planetary boundary layer in the Peruvian Amazon,
691 J. Geophys. Res. Atmospheres, 103(D19), 25519–25532, doi:10.1029/98JD01023, 1998.

692 Helmig, D., Bocquet, F., Pollmann, J. and Revermann, T.: Analytical techniques for sesquiterpene
693 emission rate studies in vegetation enclosure experiments, Atmos. Environ., 38(4), 557–572,
694 doi:10.1016/j.atmosenv.2003.10.012, 2004.

695 Hollesen, J., Buchwal, A., Rachlewicz, G., Hansen, B. U., Hansen, M. O., Stecher, O. and
696 Elberling, B.: Winter warming as an important co-driver for Betula nana growth in western
697 Greenland during the past century, in Global change biology., 2015.

698 Holst, T., Arneth, A., Hayward, S., Ekberg, A., Mastepanov, M., Jackowicz-Korczynski, M.,
699 Friborg, T., Crill, P. M. and Bäckstrand, K.: BVOC ecosystem flux measurements at a high latitude
700 wetland site, Atmospheric Chem. Phys., 10(4), 1617–1634, doi:https://doi.org/10.5194/acp-10-
701 1617-2010, 2010.

702 Holton, J. R. and Hakim, G. J.: Chapter 8 - The Planetary Boundary Layer, in An Introduction to
703 Dynamic Meteorology (Fifth Edition), edited by J. R. Holton and G. J. Hakim, pp. 255–277,
704 Academic Press, Boston., 2013.

705 Honrath, R. E. and Jaffe, D. A.: The seasonal cycle of nitrogen oxides in the Arctic troposphere at
706 Barrow, Alaska, J. Geophys. Res. Atmospheres, 97(D18), 20615–20630, doi:10.1029/92JD02081,
707 1992.

708 Hu, L., Millet, D. B., Baasandorj, M., Griffis, T. J., Turner, P., Helmig, D., Curtis, A. J. and
709 Hueber, J.: Isoprene emissions and impacts over an ecological transition region in the U.S. Upper
710 Midwest inferred from tall tower measurements, J. Geophys. Res. Atmospheres, 120(8), 3553–
711 3571, doi:10.1002/2014JD022732, 2015.

712 Isaacman-VanWertz, G., Sueper, D. T., Aikin, K. C., Lerner, B. M., Gilman, J. B., de Gouw, J. A.,
713 Worsnop, D. R. and Goldstein, A. H.: Automated single-ion peak fitting as an efficient approach
714 for analyzing complex chromatographic data, J. Chromatogr. A, 1529, 81–92,
715 doi:10.1016/j.chroma.2017.11.005, 2017.

716   Jardine, K. J., Monson, R. K., Abrell, L., Saleska, S. R., Arneth, A., Jardine, A., Ishida, F. Y.,
717   Serrano, A. M. Y., Artaxo, P., Karl, T., Fares, S., Goldstein, A., Loreto, F. and Huxman, T.:
718   Within-plant isoprene oxidation confirmed by direct emissions of oxidation products methyl vinyl
719   ketone and methacrolein, Glob. Change Biol., 18(3), 973–984, doi:10.1111/j.1365-
720   2486.2011.02610.x, 2012.

721   Kade, A., Bret-Harte, M. S., Euskirchen, E. S., Edgar, C. and Fulweber, R. A.: Upscaling of CO2
722   fluxes from heterogeneous tundra plant communities in Arctic Alaska, J. Geophys. Res.
723   Biogeosciences, 117(G4), doi:10.1029/2012JG002065, 2012.

724   Karbiwnyk, C. M., Mills, C. S., Helmig, D. and Birks, J. W.: Minimization of water vapor
725   interference in the analysis of non-methane volatile organic compounds by solid adsorbent
726   sampling, J. Chromatogr. A, 958(1–2), 219–229, doi:10.1016/s0021-9673(02)00307-2, 2002.

727   Karbiwnyk, C. M., Mills, C. S., Helmig, D. and Birks, J. W.: Use of chloroflurocarbons as internal
728   standards for the measurement of atmospheric non-methane volatile organic compounds sampled
729   onto solid adsorbent cartridges, Environ. Sci. Technol., 37(5), 1002–1007,
730   doi:10.1021/es025910q, 2003.

731   Karl, T., Potosnak, M., Guenther, A., Clark, D., Walker, J., Herrick, J. D. and Geron, C.: Exchange
732   processes of volatile organic compounds above a tropical rain forest: Implications for modeling
733   tropospheric chemistry above dense vegetation, J. Geophys. Res. Atmospheres, 109(D18),
734   doi:10.1029/2004JD004738, 2004.

735   Kramshøj, M., Vedel-Petersen, I., Schollert, M., Rinnan, Å., Nymand, J., Ro-Poulsen, H. and
736   Rinnan, R.: Large increases in Arctic biogenic volatile emissions are a direct effect of warming,
737   Nat. Geosci., 9(5), 349–352, doi:10.1038/ngeo2692, 2016.

738   Kulmala, M., Suni, T., Lehtinen, K. E. J., Maso, M. D., Boy, M., Reissell, A., Rannik, Ü., Aalto,
739   P., Keronen, P., Hakola, H., Bäck, J., Hoffmann, T., Vesala, T. and Hari, P.: A new feedback
740   mechanism linking forests, aerosols, and climate, Atmospheric Chem. Phys., 4(2), 557–562,
741   doi:https://doi.org/10.5194/acp-4-557-2004, 2004.

742   Lader, R., Walsh, J. E., Bhatt, U. S. and Bieniek, P. A.: Projections of Twenty-First-Century
743   Climate Extremes for Alaska via Dynamical Downscaling and Quantile Mapping, J. Appl.
744   Meteorol. Climatol., 56(9), 2393–2409, doi:10.1175/JAMC-D-16-0415.1, 2017.

745   Lappalainen, H. K., Sevanto, S., Bäck, J., Ruuskanen, T. M., Kolari, P., Taipale, R., Rinne, J.,
746   Kulmala, M. and Hari, P.: Day-time concentrations of biogenic volatile organic compounds in a
747   boreal forest canopy and their relation to environmental and biological factors, Atmospheric
748   Chem. Phys., 9(15), 5447–5459, doi:https://doi.org/10.5194/acp-9-5447-2009, 2009.

749   Li, T., Holst, T., Michelsen, A. and Rinnan, R.: Amplification of plant volatile defence against
750   insect herbivory in a warming Arctic tundra, Nat. Plants, 5(6), 568–574, doi:10.1038/s41477-019-
751   0439-3, 2019.

752 Lim, H.-J., Carlton, A. G. and Turpin, B. J.: Isoprene Forms Secondary Organic Aerosol through
753 Cloud Processing: Model Simulations, Environ. Sci. Technol., 39(12), 4441–4446,
754 doi:10.1021/es048039h, 2005.

755 Lindfors, V., Laurila, T., Hakola, H., Steinbrecher, R. and Rinne, J.: Modeling speciated terpenoid
756 emissions from the European boreal forest, Atmos. Environ., 34(29), 4983–4996,
757 doi:10.1016/S1352-2310(00)00223-5, 2000.

758 Lindwall, F., Faubert, P. and Rinnan, R.: Diel Variation of Biogenic Volatile Organic Compound
759 Emissions- A field Study in the Sub, Low and High Arctic on the Effect of Temperature and Light,
760 PLOS ONE, 10(4), e0123610, doi:10.1371/journal.pone.0123610, 2015.

761 Lindwall, F., Schollert, M., Michelsen, A., Blok, D. and Rinnan, R.: Fourfold higher tundra volatile
762 emissions due to arctic summer warming, J. Geophys. Res. Biogeosciences, 121(3), 895–902,
763 doi:10.1002/2015JG003295, 2016.

764 Liu, X., Pawliszyn, R., Wang, L. and Pawliszyn, J.: On-site monitoring of biogenic emissions from
765 Eucalyptus dunnii leaves using membrane extraction with sorbent interface combined with a
766 portable gas chromatograph system, The Analyst, 129(1), 55–62, doi:10.1039/b311998j, 2004.

767 Loreto, F. and Schnitzler, J.-P.: Abiotic stresses and induced BVOCs, Trends Plant Sci., 15(3),
768 154–166, doi:10.1016/j.tplants.2009.12.006, 2010.

769 Macias-Fauria, M., Forbes, B. C., Zetterberg, P. and Kumpula, T.: Eurasian Arctic greening
770 reveals teleconnections and the potential for structurally novel ecosystems, Nat. Clim. Change,
771 2(8), 613–618, doi:10.1038/nclimate1558, 2012.

772 Markon, C. J., Trainor, S. F. and Chapin, F. S.: The United States National Climate Assessment -
773 Alaska Technical Regional Report. [online] Available from:
774 https://pubs.usgs.gov/circ/1379/pdf/circ1379.pdf, 2012.

775 Michelsen, A., Rinnan, R. and Jonasson, S.: Two decades of experimental manipulations of heaths
776 and forest understory in the subarctic, Ambio, 41 Suppl 3, 218–230, doi:10.1007/s13280-012-
777 0303-4, 2012.

778 Millet, D. B., Alwe, H. D., Chen, X., Deventer, M. J., Griffis, T. J., Holzinger, R., Bertman, S. B.,
779 Rickly, P. S., Stevens, P. S., Léonardis, T., Locoge, N., Dusanter, S., Tyndall, G. S., Alvarez, S.
780 L., Erickson, M. H. and Flynn, J. H.: Bidirectional Ecosystem–Atmosphere Fluxes of Volatile
781 Organic Compounds Across the Mass Spectrum: How Many Matter?, ACS Earth Space Chem.,
782 doi:10.1021/acsearthspacechem.8b00061, 2018.

783 Olofsson, M., Ek-Olausson, B., Jensen, N. O., Langer, S. and Ljungström, E.: The flux of isoprene
784 from a willow coppice plantation and the effect on local air quality, Atmos. Environ., 39(11),
785 2061–2070, doi:10.1016/j.atmosenv.2004.12.015, 2005.

786 Ormeño, E., Mevy, J. P., Vila, B., Bousquet-Melou, A., Greff, S., Bonin, G. and Fernandez, C.:
787 Water deficit stress induces different monoterpene and sesquiterpene emission changes in

788 Mediterranean species. Relationship between terpene emissions and plant water potential.,
789 Chemosphere, 67(2), 276–284, 2007.

790 Ortega, J. and Helmig, D.: Approaches for quantifying reactive and low-volatility biogenic organic
791 compound emissions by vegetation enclosure techniques – Part A, Chemosphere, 72(3), 343–364,
792 doi:10.1016/j.chemosphere.2007.11.020, 2008.

793 Ortega, J., Helmig, D., Daly, R. W., Tanner, D. M., Guenther, A. B. and Herrick, J. D.: Approaches
794 for quantifying reactive and low-volatility biogenic organic compound emissions by vegetation
795 enclosure techniques – Part B: Applications, Chemosphere, 72(3), 365–380,
796 doi:10.1016/j.chemosphere.2008.02.054, 2008.

797 Overland, J. E., Wang, M., Walsh, J. E. and Stroeve, J. C.: Future Arctic climate changes:
798 Adaptation and mitigation time scales, Earths Future, 2(2), 68–74, doi:10.1002/2013EF000162,
799 2014.

800 Peñuelas, J. and Staudt, M.: BVOCs and global change, Trends Plant Sci., 15(3), 133–144,
801 doi:10.1016/j.tplants.2009.12.005, 2010.

802 Pollmann, J., Ortega, J. and Helmig, D.: Analysis of Atmospheric Sesquiterpenes: Sampling
803 Losses and Mitigation of Ozone Interferences, Environ. Sci. Technol., 39(24), 9620–9629,
804 doi:10.1021/es050440w, 2005.

805 Potosnak, M. J., Baker, B. M., LeStourgeon, L., Disher, S. M., Griffin, K. L., Bret-Harte, M. S.
806 and Starr, G.: Isoprene emissions from a tundra ecosystem, Biogeosciences, 10(2), 871–889,
807 doi:10.5194/bg-10-871-2013, 2013.

808 Pressley, S., Lamb, B., Westberg, H., Flaherty, J., Chen, J. and Vogel, C.: Long-term isoprene flux
809 measurements above a northern hardwood forest, J. Geophys. Res. Atmospheres, 110(D7),
810 doi:10.1029/2004JD005523, 2005.

811 Raynolds, M. K., Walker, D. A., Balser, A., Bay, C., Campbell, M., Cherosov, M. M., Daniëls, F.
812 J. A., Eidesen, P. B., Ermokhina, K. A., Frost, G. V., Jedrzejek, B., Jorgenson, M. T., Kennedy,
813 B. E., Kholod, S. S., Lavrinenko, I. A., Lavrinenko, O. V., Magnússon, B., Matveyeva, N. V.,
814 Metúsalemsson, S., Nilsen, L., Olthof, I., Pospelov, I. N., Pospelova, E. B., Pouliot, D., Razzhivin,
815 V., Schaepman-Strub, G., Šibík, J., Telyatnikov, M. Yu. and Troeva, E.: A raster version of the
816 Circumpolar Arctic Vegetation Map (CAVM), Remote Sens. Environ., 232, 111297,
817 doi:10.1016/j.rse.2019.111297, 2019.

818 Rinnan, R., Rinnan, Å., Faubert, P., Tiiva, P., Holopainen, J. K. and Michelsen, A.: Few long-term
819 effects of simulated climate change on volatile organic compound emissions and leaf chemistry of
820 three subarctic dwarf shrubs, Environ. Exp. Bot., 72(3), 377–386,
821 doi:10.1016/j.envexpbot.2010.11.006, 2011.

822 Rinnan, R., Steinke, M., McGenity, T. and Loreto, F.: Plant volatiles in extreme terrestrial and
823 marine environments, Plant Cell Environ., 37(8), 1776–1789, doi:10.1111/pce.12320, 2014.

824 Rinne, H. J. I., Guenther, A. B., Greenberg, J. P. and Harley, P. C.: Isoprene and monoterpene
825 fluxes measured above Amazonian rainforest and their dependence on light and temperature,
826 Atmos. Environ., 36(14), 2421–2426, doi:10.1016/S1352-2310(01)00523-4, 2002.

827 Rinne, J., Bäck, J. and Hakola, H.: Biogenic volatile organic compound emissions from the
828 Eurasian taiga: current knowledge and future directions, , 14, 20, 2009.

829 Rivera-Rios, J. C., Nguyen, T. B., Crounse, J. D., Jud, W., Clair, J. M. S., Mikoviny, T., Gilman,
830 J. B., Lerner, B. M., Kaiser, J. B., Gouw, J. de, Wisthaler, A., Hansel, A., Wennberg, P. O.,
831 Seinfeld, J. H. and Keutsch, F. N.: Conversion of hydroperoxides to carbonyls in field and
832 laboratory instrumentation: Observational bias in diagnosing pristine versus anthropogenically
833 controlled atmospheric chemistry, Geophys. Res. Lett., 41(23), 8645–8651,
834 doi:10.1002/2014GL061919, 2014.

835 Ruuskanen, T. M., Kolari, P., Bäck, J., Kulmala, M., Rinne, J., Hakola, H., Taipale, R., Raivonen,
836 M., Altimir, N. and Hari, P.: On-line field measurements of monoterpene emissions from Scots
837 pine by proton-transfer-reaction mass spectrometry, Boreal Environ. Res., 10(6), 553–567, 2005.

838 Sasaki, K., Saito, T. and Lamsa, M.: Plants utilize isoprene emission as a thermotolerance
839 mechanism, Plant Cell Physiol., 48, 1254–1262, 2007.

840 Scanlon, J. T. and Willis, D. E.: Calculation of Flame Ionization Detector Relative Response
841 Factors Using the Effective Carbon Number Concept, J. Chromatogr. Sci., 23(8), 333–340,
842 doi:10.1093/chromsci/23.8.333, 1985.

843 Schollert, M., Burchard, S., Faubert, P., Michelsen, A. and Rinnan, R.: Biogenic volatile organic
844 compound emissions in four vegetation types in high arctic Greenland, Polar Biol., 37(2), 237–
845 249, doi:10.1007/s00300-013-1427-0, 2014.

846 Schollert, M., Kivimäenpää, M., Valolahti, H. M. and Rinnan, R.: Climate change alters leaf
847 anatomy, but has no effects on volatile emissions from arctic plants, Plant Cell Environ., 38(10),
848 2048–2060, doi:10.1111/pce.12530, 2015.

849 Shaver, G. R. and Chapin, F. S.: Production: Biomass Relationships and Element Cycling in
850 Contrasting Arctic Vegetation Types, Ecol. Monogr., 61(1), 1–31, doi:10.2307/1942997, 1991.

851 Sindelarova, K., Granier, C., Bouarar, I., Guenther, A., Tilmes, S., Stavrakou, T., Müller, J.-F.,
852 Kuhn, U., Stefani, P. and Knorr, W.: Global data set of biogenic VOC emissions calculated by the
853 MEGAN model over the last 30 years, Atmospheric Chem. Phys., 14(17), 9317–9341,
854 doi:https://doi.org/10.5194/acp-14-9317-2014, 2014.

855 Sistla, S. A., Moore, J. C., Simpson, R. T., Gough, L., Shaver, G. R. and Schimel, J. P.: Long-term
856 warming restructures Arctic tundra without changing net soil carbon storage, Nature, 497(7451),
857 615–618, doi:10.1038/nature12129, 2013.

858 Spirig, C., Guenther, A., Greenberg, J. P., Calanca, P. and Tarvainen, V.: Tethered balloon
859 measurements of biogenic volatile organic compounds at a Boreal forest site, Atmospheric Chem.
860 Phys., 4(1), 215–229, doi:https://doi.org/10.5194/acp-4-215-2004, 2004.

861 Sturm, M., Racine, C. and Tape, K.: Climate change: Increasing shrub abundance in the Arctic,
862 Nature, 411(6837), 546–547, doi:10.1038/35079180, 2001.

863 Sullivan, P. F., Sommerkorn, M., Rueth, H. M., Nadelhoffer, K. J., Shaver, G. R. and Welker, J.
864 M.: Climate and species affect fine root production with long-term fertilization in acidic tussock
865 tundra near Toolik Lake, Alaska, Oecologia, 153(3), 643–652, doi:10.1007/s00442-007-0753-8,
866 2007.

867 Survey: Maps - Toolik Lake Area Vegetation, [online] Available from:
868 http://www.arcticatlas.org/maps/themes/tl5k/tl5kvg (Accessed 30 September 2019), 2012.

869 Tang, J., Schurgers, G., Valolahti, H., Faubert, P., Tiiva, P., Michelsen, A. and Rinnan, R.:
870 Challenges in modelling isoprene and monoterpene emission dynamics of Arctic plants: a case
871 study from a subarctic tundra heath, Biogeosciences, 13(24), 6651–6667,
872 doi:https://doi.org/10.5194/bg-13-6651-2016, 2016.

873 Tape, K., Sturm, M. and Racine, C.: The evidence for shrub expansion in Northern Alaska and the
874 Pan-Arctic, Glob. Change Biol., 12(4), 686–702, doi:10.1111/j.1365-2486.2006.01128.x, 2006.

875 Tarvainen, V., Hakola, H., Rinne, J., HellàN, H. and Haapanala, S.: Towards a comprehensive
876 emission inventory of terpenoids from boreal ecosystems, Tellus B Chem. Phys. Meteorol., 59(3),
877 526–534, doi:10.1111/j.1600-0889.2007.00263a.x, 2007.

878 Tiiva, P., Faubert, P., Michelsen, A., Holopainen, T., Holopainen, J. K. and Rinnan, R.: Climatic
879 warming increases isoprene emission from a subarctic heath, New Phytol., 180(4), 853–863,
880 doi:10.1111/j.1469-8137.2008.02587.x, 2008.

881 Toolik Field Station Environmental Data Center: Toolik Field Station::Weather Data Query,
882 [online] Available from: https://toolik.alaska.edu/edc/abiotic_monitoring/data_query.php
883 (Accessed 30 September 2019), 2019.

884 Tsigaridis, K. and Kanakidou, M.: Secondary organic aerosol importance in the future atmosphere,
885 Atmos. Environ., 41(22), 4682–4692, doi:10.1016/j.atmosenv.2007.03.045, 2007.

886 Unger, N.: Human land-use-driven reduction of forest volatiles cools global climate, Nat. Clim.
887 Change, 4(10), 907–910, doi:10.1038/nclimate2347, 2014.

888 Valolahti, H., Kivimäenpää, M., Faubert, P., Michelsen, A. and Rinnan, R.: Climate change-
889 induced vegetation change as a driver of increased subarctic biogenic volatile organic compound
890 emissions, Glob. Change Biol., 21(9), 3478–3488, doi:10.1111/gcb.12953, 2015.

891 Van Dam, B., Helmig, D., Burkhart, J. F., Obrist, D. and Oltmans, S. J.: Springtime boundary layer
892 O3 and GEM depletion at Toolik Lake, Alaska, J. Geophys. Res. Atmospheres, 118(8), 3382–
893 3391, doi:10.1002/jgrd.50213, 2013.

894 Van Dam, B., Helmig, D., Doskey, P. V. and Oltmans, S. J.: Summertime surface O3 behavior
895 and deposition to tundra in the Alaskan Arctic, J. Geophys. Res. Atmospheres, 121(13), 8055–
896 8066, doi:10.1002/2015JD023914, 2016.

897 Vedel-Petersen, I., Schollert, M., Nymand, J. and Rinnan, R.: Volatile organic compound emission
898 profiles of four common arctic plants, Atmos. Environ., 120, 117–126,
899 doi:10.1016/j.atmosenv.2015.08.082, 2015.

900 Walker, M. D., Walker, D. A. and Auerbach, N. A.: Plant communities of a tussock tundra
901 landscape in the Brooks Range Foothills, Alaska, J. Veg. Sci., 5(6), 843–866,
902 doi:10.2307/3236198, 1994.

903 Wang, J.-L., Chew, C., Chen, S.-W. and Kuo, S.-R.: Concentration Variability of Anthropogenic
904 Halocarbons and Applications as Internal Reference in Volatile Organic Compound
905 Measurements, Environ. Sci. Technol., 34(11), 2243–2248, doi:10.1021/es991128n, 2000.

906 Zini, C. A., Augusto, F., Christensen, T. E., Smith, B. P., Caramão, E. B. and Pawliszy, J.:
907 Monitoring biogenic volatile compounds emitted by Eucalyptus citriodora using SPME, Anal.
908 Chem., 73(19), 4729–4735, doi:10.1021/ac0103219, 2001.

909

910   Table 1: Year 2017 median relative percent cover of plant species in moist acidic tundra long-term

911   ecological research (LTER) experimental control plots at Toolik Field Station. The last column indicates

912   whether plant species were present in surface or bag enclosure experiments in this study.

Plant name	Relative land surface cover in moist acidic tundra (%) (Gough, 2019)	Present in surface or bag enclosures
Andromeda polifolia	0.6	yes
Betula nana	14.4	yes
Carex bigelowii	1.0	yes
Cassiope tetragona	2.0	yes
Empetrum nigrum	3.8	yes
Eriophorum vaginatum	8.6	yes
Ledum palustre	10.5	yes
Mixed Lichens	2.1	yes
Mixed moss	6.0	yes
Pedicularis lapponica	0.6	no
Polygonum bistorta	0.6	no
Rubus chamaemorus	20.2	no
Salix pulchra	4.9	yes
Vaccinium uliginosum	1.9	yes
Vaccinium vitis-idaea	6.6	yes

913

914

915

916

917

918 Table 2: Average mixings ratios with standard deviation, along with minimum (min) and maximum (max)
919 values and quantification frequency (QF) of the measured monoterpenes in ambient air. LOQ stands for
920 limit of quantification. For values lower than the LOQ, mixing ratios equal to half of the LOQ were used
921 to calculate the mean.

	mean ± standard deviation (pptv)	Min (pptv)	Max (pptv)	QF (%)
α-pinene	11.7 ± 8.1	< LOQ	61.6	88
camphene	< LOQ	< LOQ	21.9	11
sabinene	< LOQ	< LOQ	34.2	11
p-cymene	2.0 ± 1.9	< LOQ	12.3	32
limonene	< LOQ	< LOQ	2.9	< 1

922

923

924

925

926

927

928

929

930

931

932

933

934

935

936 Table 3: Isoprene and monoterpenes (sum of α-pinene, β-pinene, limonene, and 1,8-cineole) surface

937 emission rates per vegetation type. Miscellaneous refers to a mix of different species, including lichens and

938 moss tundra (see Fig.S.I.3-15). Daytime refers to 10 am-8 pm, midday to 11 am-2 pm, and nighttime to 11

939 pm-5 am (Alaska Standard Time). The values in brackets represent the average enclosure temperature for

940 each emission rate.

|	mean ± standard deviation (μgC/m^2/h)	daytime mean ± standard deviation (μgC/m^2/h)	midday mean ± standard deviation (μgC/m^2/h)	nighttime mean ± standard deviation (μgC/m^2/h)
isoprene				
Salix spp.	149 ± 327 [17.6°C]	232 ± 400 [23.9°C]	334 ± 473 [27.0°C]	7 ± 10 [8.0°C]
Betula spp.	12 ± 30 [13.7°C]	19 ± 38 [17.4°C]	28 ± 37 [20.1°C]	5 ± 14 [5.8°C]
Miscellaneous	38 ± 81 [11.8°C]	57 ± 100 [14.8°C]	104 ± 135 [16.2°C]	21 ± 64 [8.2°C]
monoterpenes				
Salix spp.	0.8 ± 1.3 [17.6°C]	1.1 ± 1.5 [23.9°C]	1.4 ± 1.7 [27.0°C]	0.4 ± 1.0 [8.0°C]
Betula spp.	0.5 ± 0.6 [13.7°C]	0.7 ± 0.7 [17.4°C]	1.0 ± 0.8 [20.1°C]	0.2 ± 0.2 [5.8°C]
Miscellaneous	1.1 ± 1.4 [11.8°C]	1.3 ± 1.6 [14.8°C]	1.7 ± 2.0 [16.2°C]	1.0 ± 1.4 [8.2°C]

941

942

943

944

945

946

947
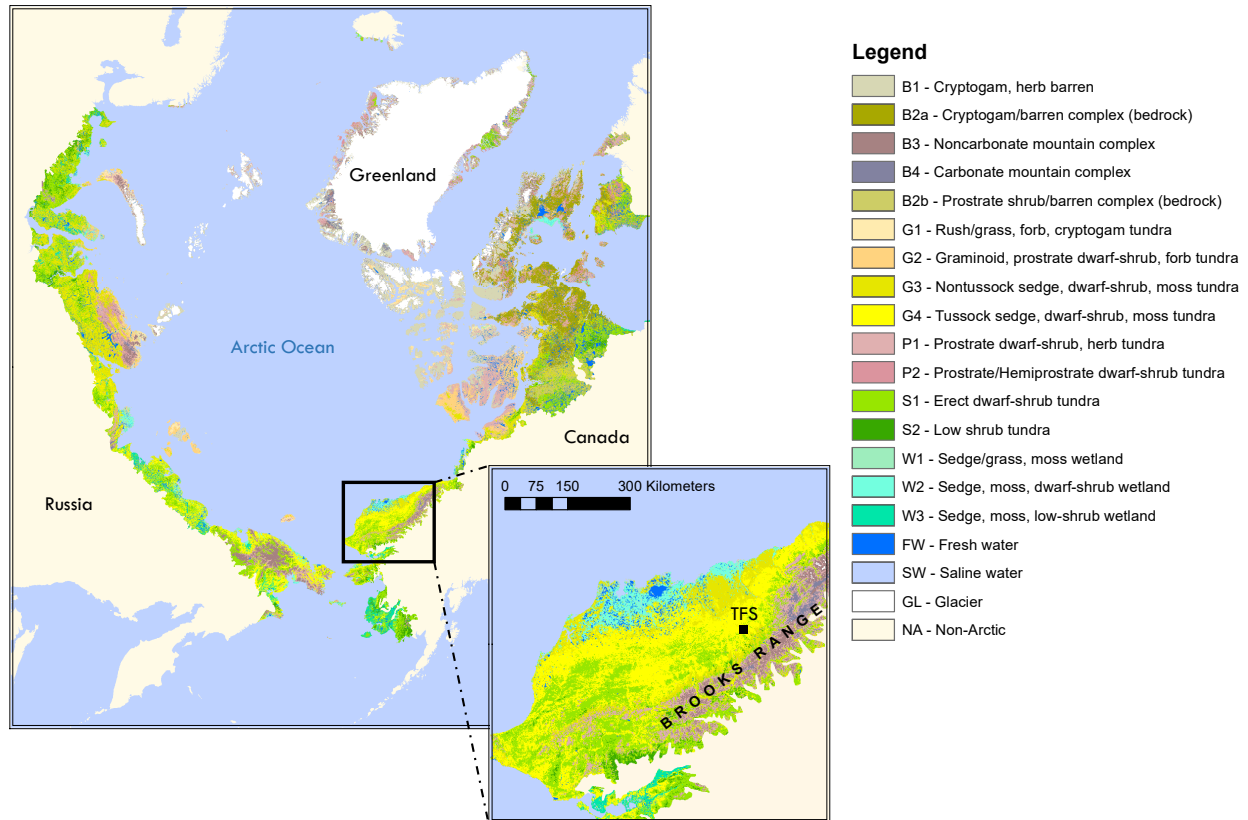
Figure 1: Location of Toolik Field Station (TFS) on the north flanks of the Brooks Range in northern Alaska
along with arctic vegetation type. This Figure was made using the raster version of the Circumpolar Arctic
Vegetation Map prepared by Raynolds et al. (2019) and publicly available at www.geobotany.uaf.edu.
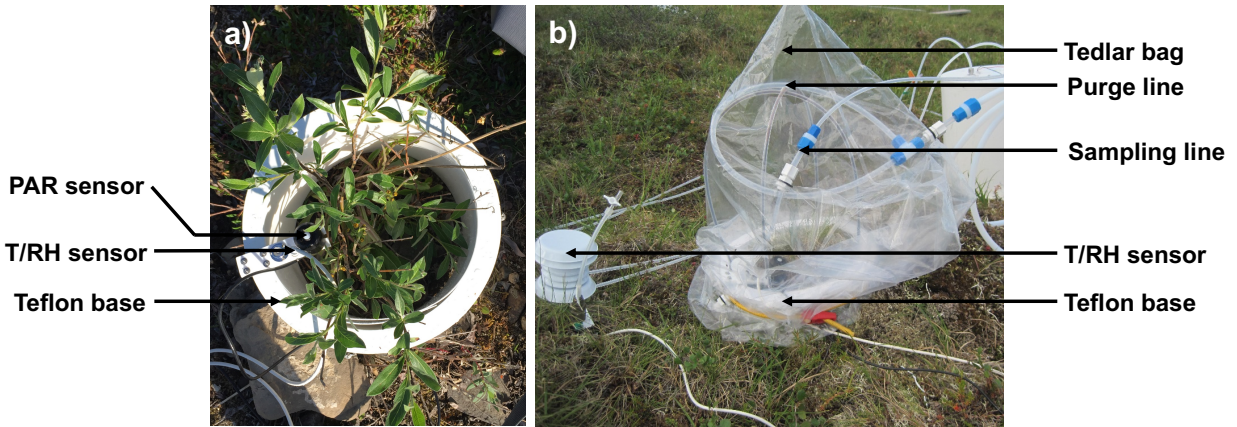
951

952

953

954

955

956

957

958

959

960

961

962   Figure 2: Photographs of a surface enclosure experiment setup at Toolik Field Station, Alaska. a) The first
963   step of the installation consisted in positioning the Teflon® base around the vegetation of interest along
964   with temperature (T), relative humidity (RH), and photosynthetically active radiation (PAR) sensors. b)
965   The second step consisted in positioning the Tedlar® bag around the base. The bag was connected to a
966   purge air and a sampling line. An additional T/RH sensor was also positioned outside the bag.

967

968

969

970

971

972

973

974

975

976

977

978

979

980
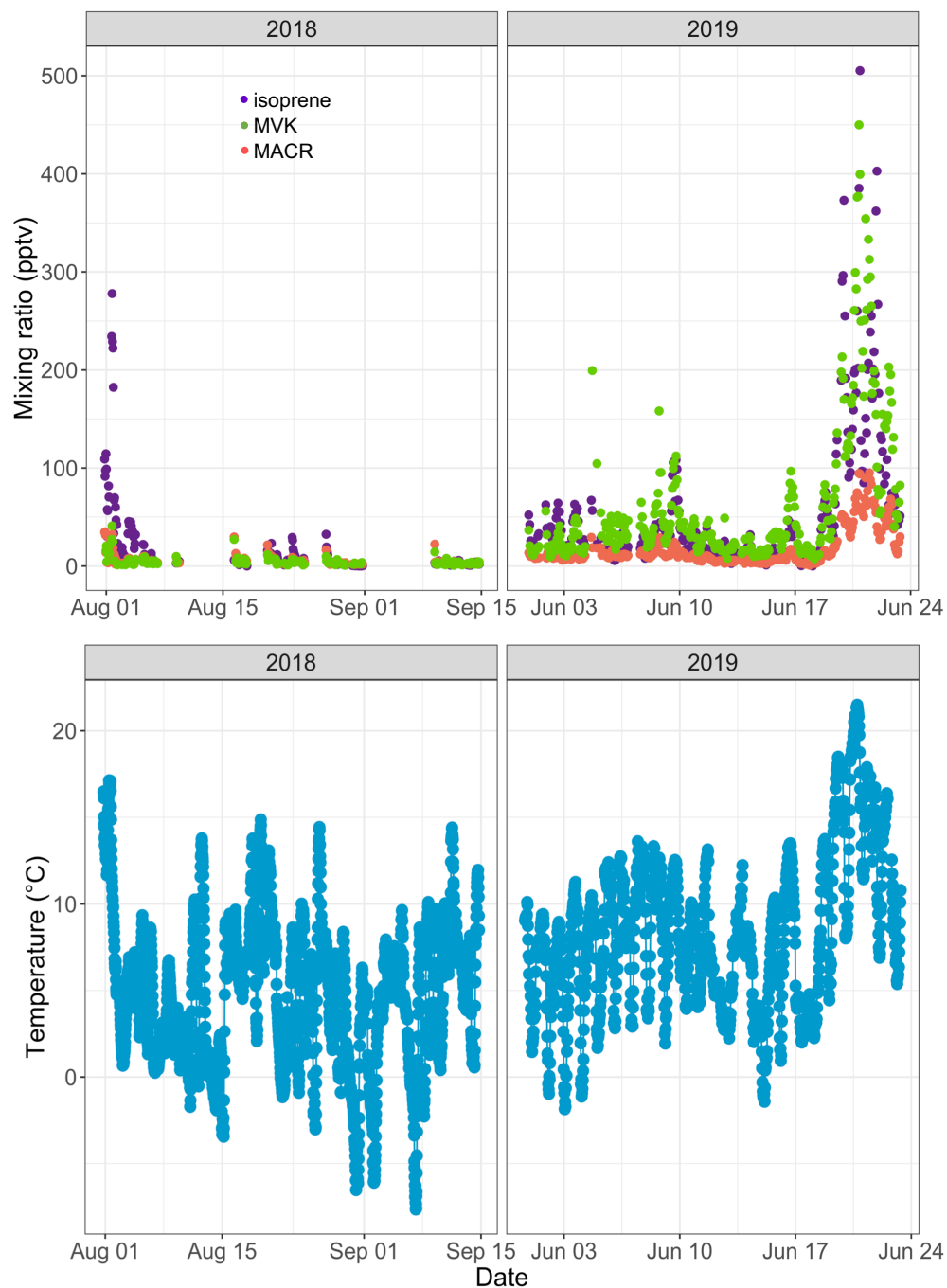
Figure 3: Time-series of isoprene (purple), methylvinylketone (MVK, green), and methacrolein (MACR, salmon) mixing ratios (in pptv) in ambient air at Toolik Field station (top panels) and of 30-min-averaged ambient temperature (in °C) at 4 meters above ground level (bottom panels).
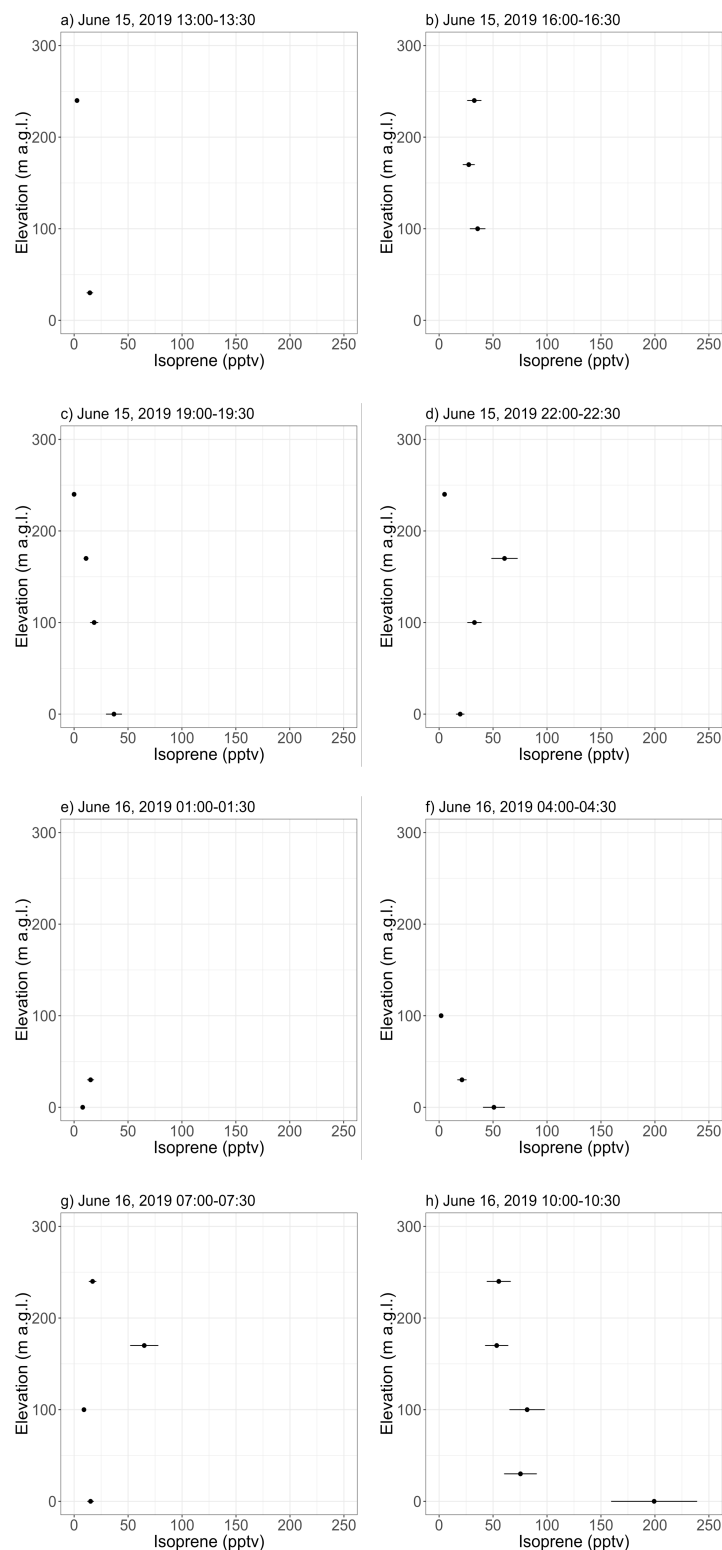
984

985

986
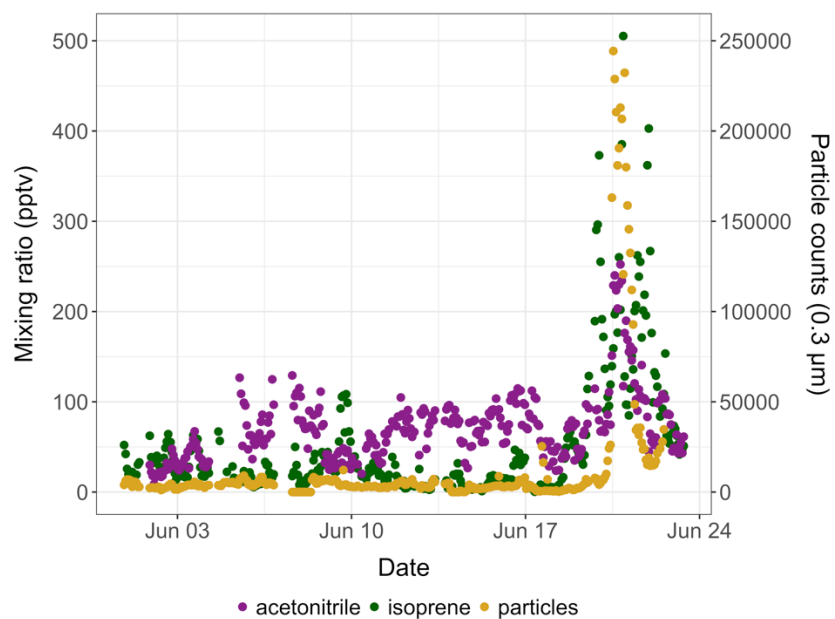
987   Figure 4: Time-series of isoprene (green) and acetonitrile (purple) mixing ratios (in pptv) and of 0.3 µm

988   particle counts (yellow) in ambient air at Toolik Field station in June 2019.

989

990

991

992

993

994

995

996

Figure 5: Vertical profiles of isoprene mixing ratios as inferred from 30-min samples collected with a
tethered balloon. The error bars show the analytical uncertainty for isoprene (20 %). Samples with an
isoprene mixing ratio lower than blanks were discarded. Hours are in Alaska Standard Time (UTC-9).

1000
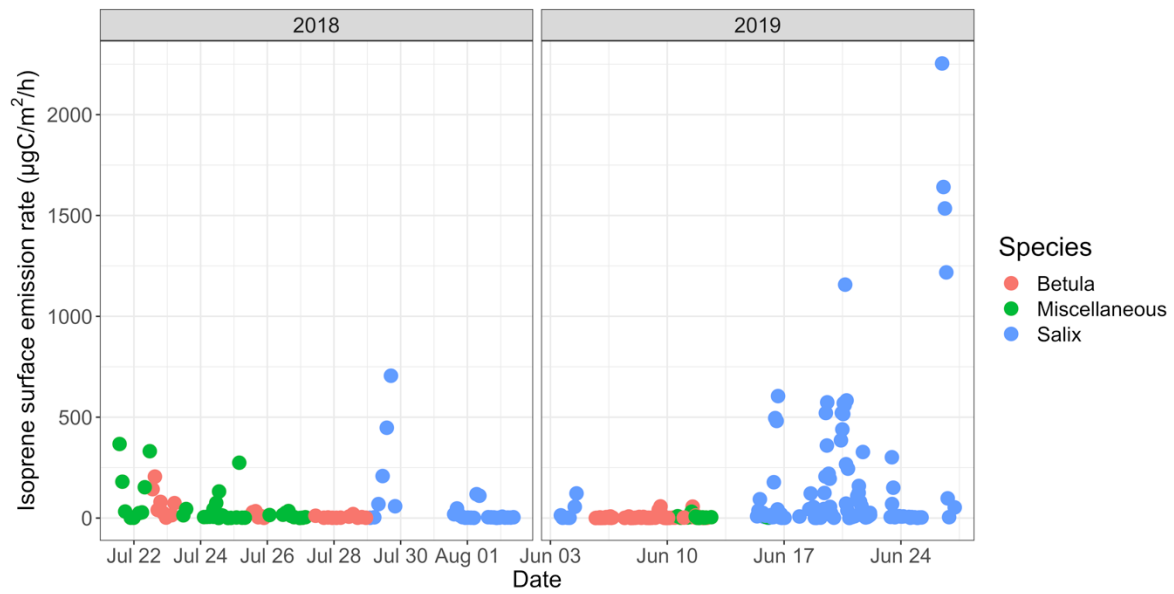
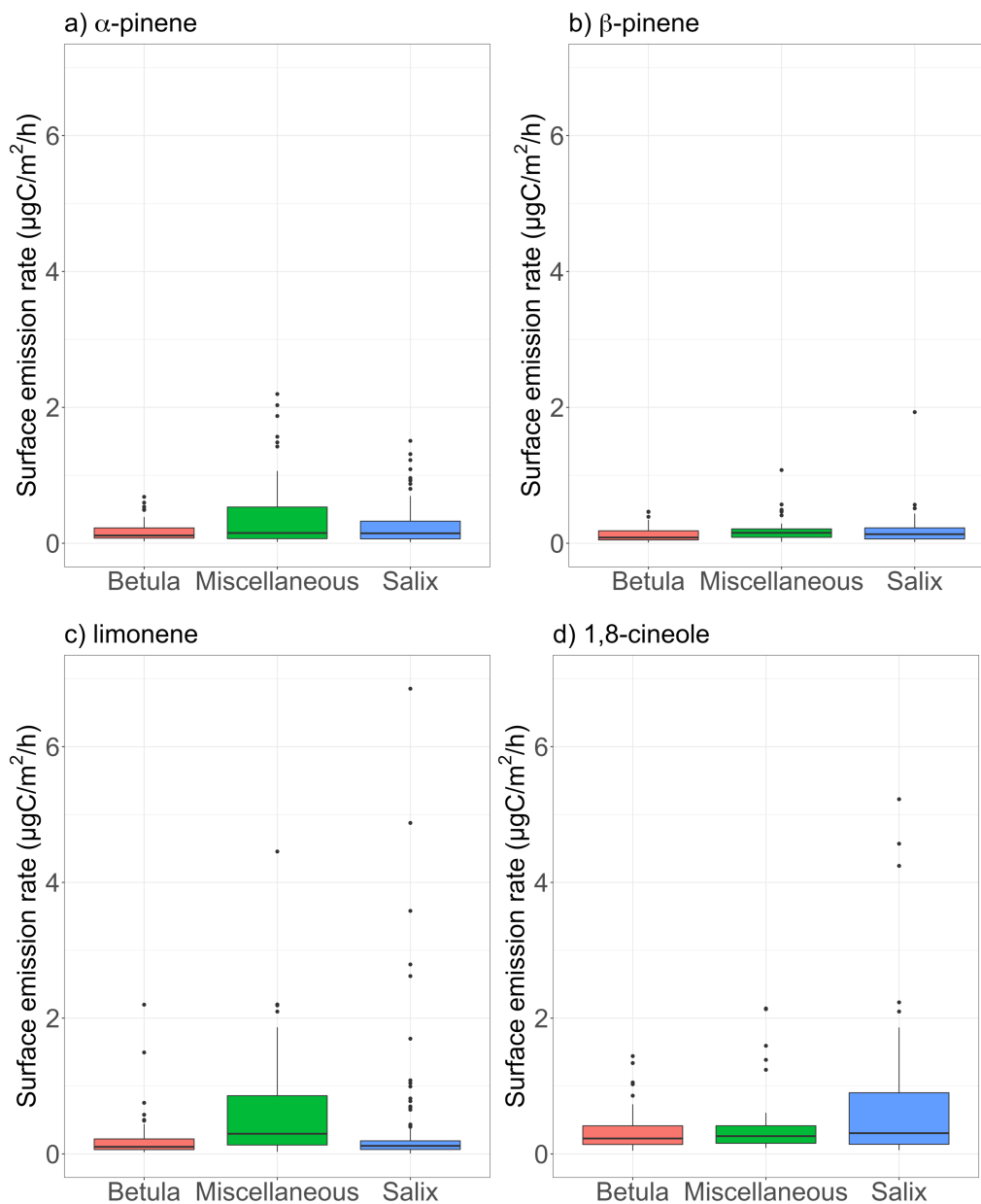1001   Figure 6: Time-series of isoprene surface emission rates (in $\mu gC/m^2/h$) for different vegetation types.

1002

1003

1004

1005

1006

1007

1008

1009

1010

1011

1012

1013   Figure 7: Surface emission rates of various monoterpenes (in µgC/m^2/h) for different vegetation types. The

1014   lower and upper hinges correspond to the first and third quartiles. The upper (lower) whisker extends from

1015   the hinge to the largest (smallest) value no further than $1.5 \times IQR$ from the hinge, where IQR is the inter-

1016   quartile range (i.e., the distance between the first and third quartiles). The notches extend $1.58 \times IQR/\sqrt{n}$

1017   and give a ~95% confidence interval for medians.
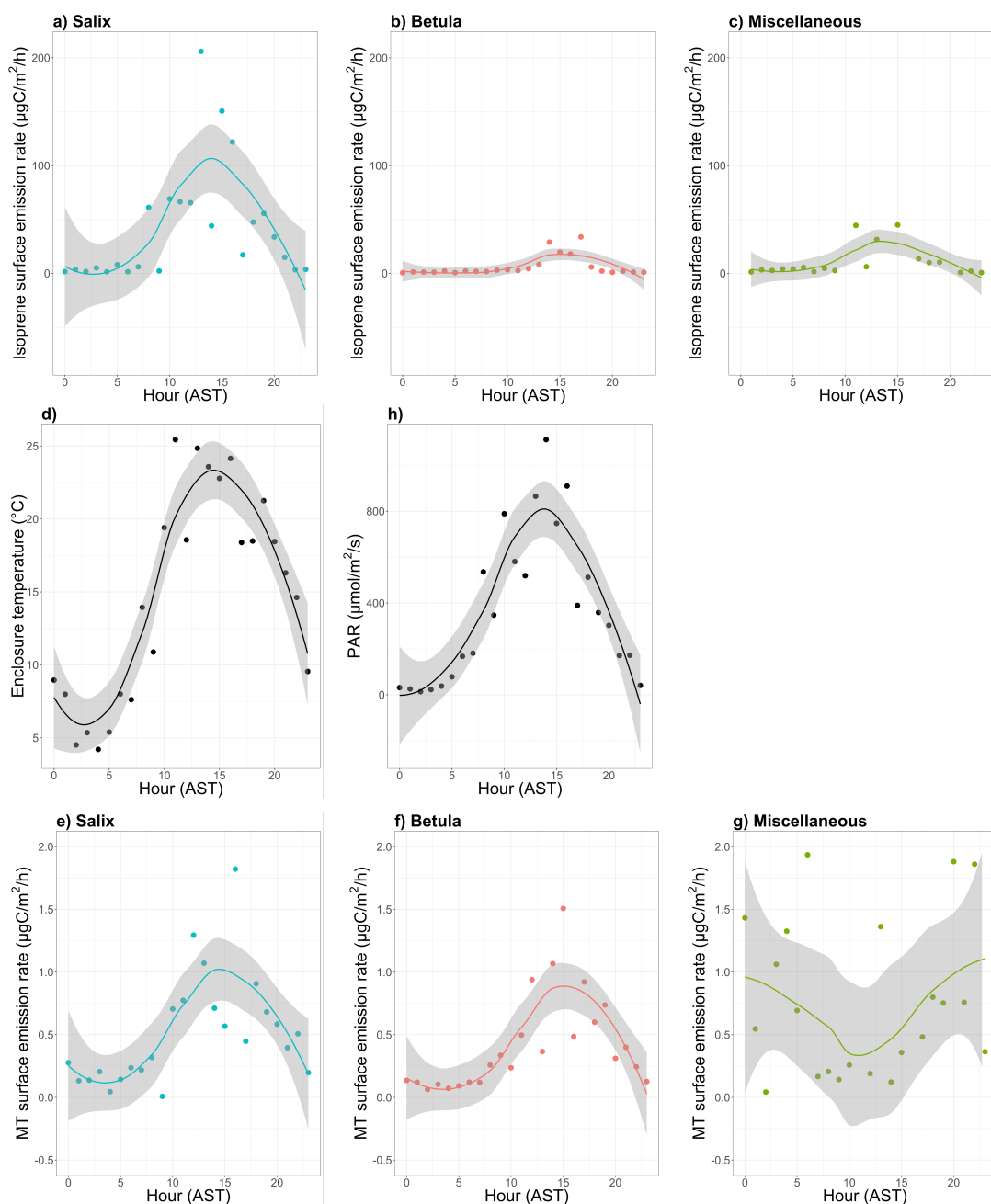
1018

1019

Figure 8: Mean diurnal cycle of isoprene (a-c) and monoterpenes (MT; e-g) surface emission rates (in μgC/m²/h – note the difference scale on the y-axis), d) enclosure temperature (in °C), and h) enclosure photosynthetically active radiation (PAR in μmol/m²/s). The dots represent the hourly means. The line is the smoothed conditional mean while the grey shaded region indicates the 95% confidence interval. Hours are in Alaska Standard Time (UTC-9) and correspond to the end of the 2-hr sampling period for isoprene and MT emission rates. MT corresponds here to the sum of α-pinene, β-pinene, limonene, and 1,8-cineole.

1026
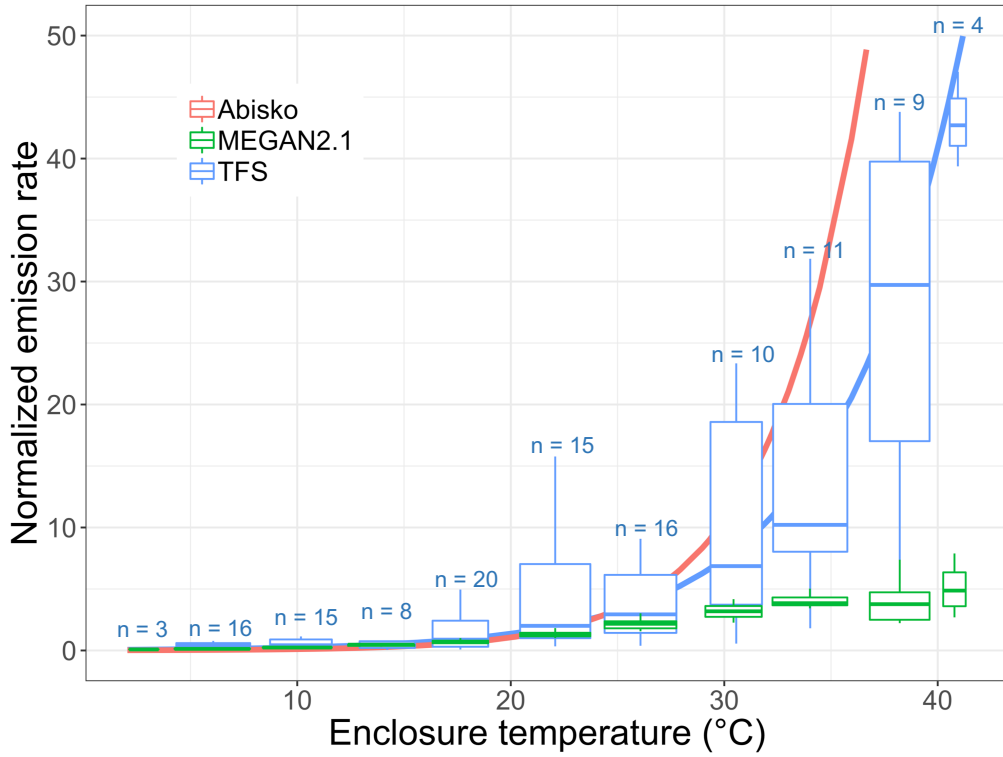
Figure 9: Normalized isoprene surface emission rate (emissions at 20°C set equal to 1.0) as a function of enclosure temperature (in °C). This figure shows the response to temperature as observed at Toolik Field Station (TFS, in blue) and Abisko, Sweden (in pink; Tang et al., 2016), and as parameterized in MEGAN2.1 (in green). The blue solid line is the exponential fit at TFS. n denotes the number of measurements in each enclosure temperature bin. It should be noted that the enclosure temperature was on average 5-6°C warmer than ambient air due to greenhouse heating.